Current Single Event Effects and Radiation Damage Results for Candidate Spacecraft Electronics

Martha V. O'Bryan[1], *Member, IEEE,* Kenneth A. LaBel[2], *Member, IEEE,* Robert A. Reed[2], *Member, IEEE,* Ray L. Ladbury[3], *Member, IEEE,* James W. Howard Jr.[4], *Senior Member, IEEE,* Scott D. Kniffin[3], *Member, IEEE,* Christian Poivey[5], *Member, IEEE,* Stephen P. Buchner[6], *Member, IEEE,* John P. Bings[7], Jeff L. Titus[7], *Senior Member, IEEE,* Steven D. Clark[7], *Member, IEEE,* Thomas L. Turflinger[7], *Member, IEEE,* John Seiler[7], Christina M. Seidleck[1], Cheryl J. Marshall[2], *Member, IEEE,* Paul W. Marshall[8], *Member, IEEE,* Hak S. Kim[4], Donald K. Hawkins[2], Martin A. Carts[1], James D. Forney[4], Anthony B. Sanders[2], Tim Irvin, Stephen R. Cox[2], Zoran A Kahric, and Christopher Palor[3]

1. Raytheon Information Technology & Scientific Services, Lanham, MD 20706-4392
2. NASA/GSFC, Code 561.4, Greenbelt, MD 20771
3. Orbital Sciences Corporation, McLean, VA
4. Jackson & Tull Chartered Engineers, Washington, D. C. 20018
5. SGT, Greenbelt, MD 20770
6. QSS, Lanham, MD 20706
7. NAVSEA Crane - Surface Warfare Center Division, Crane, IN 47522
8. Consultant

Abstract-- We present data on the vulnerability of a variety of candidate spacecraft electronics to proton and heavy ion induced single event effects, total ionizing dose and proton-induced damage. Devices tested include optoelectronics, digital, analog, linear bipolar, hybrid devices, Analog-to-Digital Converters (ADCs), Digital-to-Analog Converters (DACs), and DC-DC converters, among others.

I. INTRODUCTION

As spacecraft designers use increasing numbers of commercial and emerging technology devices to meet stringent performance, economic and schedule requirements, ground-based testing of such devices for susceptibility to single event effects (SEE), total ionizing dose (TID), and proton-induced damage has assumed ever greater importance.

Manuscript received July X, 2002. (Write the date on which you submitted your paper for review.) The work presented is sponsored by NASA Electronic Parts and Packaging (NEPP) Program's Electronics Radiation Characterization (ERC) Project, Defense Threat Reduction Agency (DTRA) under IACRO 01-4050/0001278, NASA Remote Exploration and Experimentation (REE) Project and NASA Flight Projects.

M. V. O'Bryan is with Raytheon Information Technology & Scientific Services, Lanham, MD 20706-4392 (telephone: 301-286-1412, e-mail: martha.obryan@gsfc.nasa.gov).

Kenneth A. LaBel is with NASA/GSFC, Code 562, Greenbelt, MD 20771 USA (telephone: 301-286-9936, e-mail: ken.label@gsfc.nasa.gov).

Robert A Reed is with NASA/GSFC, Code 562, Greenbelt, MD 20771 USA, (telephone: 301-286-2153, e-mail: robert.reed@gsfc.nasa.gov).

The studies discussed here were undertaken to establish the sensitivities of candidate spacecraft electronics to heavy ion and proton-induced single event upsets (SEU), single event latchup (SEL), single event transient (SET), TID and proton damage (ionizing and non-ionizing).

II. TEST TECHNIQUES AND SETUP

A. Test Facilities

All SEE and proton-induced damage tests were performed between February 2001 and February 2002. Heavy Ion experiments were conducted at the Brookhaven National Laboratories (BNL) Single Event Upset Test Facility (SEUTF) and at Texas A&M University Cyclotron (TAMU). The SEUTF uses a twin Tandem Van De Graaf accelerator while the TAMU facility uses an 88" Cyclotron. Both facilities are suitable for providing a variety of ions over a range of energies for testing. At both facilities, test boards containing the device under test (DUT) were mounted in the test area. For heavy ions, the DUT was irradiated with ions with linear energy transfers (LETs) ranging from 0.59 to 120 MeV•cm^2/mg, with fluences from 1×10^5 to 1×10^8 particles/cm^2. Fluxes ranged from 1×10^2 to 5×10^5 particles/cm^2 per second, depending on the device sensitivity. Representative ions used are listed in Table I. LETs between the values listed were obtained by changing the angle of incidence of the ion beam on the DUT, thus changing the path length of the ion through the DUT. Energies and LETs available varied slightly from one test date to another.

Proton SEE and damage tests were performed at three facilities: the University of California Davis (UCD) Crocker Nuclear Laboratory (CNL), Tri-University Meson Facility (TRIUMF), and the Indiana University Cyclotron Facility (IUCF). Proton test energies incident on the DUT are listed in Table II. Typically, the DUT was irradiated to a fluence from $1x10^{10}$ to $1x10^{11}$ particles/cm^2, with fluxes on the order of $1x10^8$ particles/cm^2 per second.

The pulsed laser facility at the Naval Research Laboratory was used to generate Single Event Transients (SETs) in integrated circuits. The laser light used had a wavelength of 590 nm that resulted in a skin depth (depth at which the light intensity decreased to 1/e - or about 37% - of its intensity at the surface) of 2 microns.

TID testing was performed using a Co-60 source at the Goddard Space Flight Center Radiation Effects Facility (GSFC REF). The source is capable of delivering a dose rate of 0.5 Rad(Si)/s, with dosimetry being performed by an ion chamber probe.

TID testing was also performed using a Co-60 source at NAVSEA Crane Surface Warfare Center Division (NAVSEA) Shepherd Model 484 Cobalt-60 Tunnel Irradiator Test Facility. The source is capable of delivering dose rates between 0.8 rad(Si)/sec and 49.5 rad(Si)/sec.

TABLE I: HEAVY ION TEST FACILITIES AND TEST HEAVY IONS

	Ion	Energy, MeV	LET in Si, MeV•cm^2/mg	Range in Si, µm
BNL	C^{12}	102	1.42	193
	O^{16}	131	2.53	145
	F^{19}	145	3.31	126
	Si^{28}	203	7.55	85.3
	Cl^{35}	224	11.1	68.5
	Ti^{48}	253	18.1	53.2
	Ni^{58}	280	26.3	44.3
	Ge^{72}	290	32.7	40.0
	Br^{79}	305	36.9	38.7
	I^{127}	370	60.1	34.3
TAMU	Ne^{20}	298	2.5	331.0
	Ar^{40}	599	7.4	243.7
	Kr^{84}	1260	25.1	154
	Xe^{29}	1935	47.1	127
	Au^{197}	390	84.1	30.2
	* O^{16}	880	0.59	3607
	* Ar^{40}	1980	3.0	1665
	* 55 MeV per nucleon tune			

Table II: Proton Test Facilities and Particles

Facility	Particle	Particle Energy, (MeV)
University of California at Davis (UCD) Crocker Nuclear Laboratory (CNL)	Proton	26.6-63
Tri-University Meson Facility (TRIUMF)	Proton	50-500
Indiana University Cyclotron Facility (IUCF)	Proton	54-197

Table III: Other Test Facilities

Naval Research Laboratory (NRL) Pulsed Laser SEE Test Facility Laser: 590 nm, 3 ps pulse width, beam spot size ~1.5 µm
NAVSEA Crane Surface Warfare Center Division (NAVSEA) Shepherd Model 484 Cobalt-60 Tunnel Irradiator Test Facility
Goddard Space Flight Center Radiation Effects Facility (GSFC REF)

B. Test Method

Unless otherwise noted, all tests were performed at room temperature and with nominal power supply voltages.

1) SEE Testing - Heavy Ion

Depending on the DUT and the test objectives, one or more of three SEE test methods were used:

Dynamic – the DUT was exercised continually while being exposed to the beam. The errors were counted, generally by comparing DUT output to an unirradiated reference device or other expected output. In some cases, the effects of clock speed or device modes were investigated. Results of such tests should be applied with caution because device modes and clock speed can affect SEE results.

Static – the DUT was loaded prior to irradiation; data were retrieved and errors were counted after irradiation.

Biased (SEL only) – the DUT was biased and clocked while I_{CC} (power consumption) was monitored for SEL or other destructive effects. In some SEL tests, functionality was also monitored.

In SEE experiments, DUTs were monitored for soft errors, such as SEUs and for hard errors, such as SEL. Detailed descriptions of the types of errors observed are noted in the individual test results.

SET testing was performed using a high-speed oscilloscope. Individual criteria for SETs are specific to the device being tested. Please see the individual test reports for details. [1]

Heavy ion SEE sensitivity experiments include measurement of the saturation cross sections and the Linear Energy Transfer (LET_{th}) threshold (the minimum LET value necessary to cause an effect at a fluence of $1x10^7$ particles/cm^2).

2) SEE Testing - Proton

Proton SEE tests were performed in a manner similar to heavy ion exposures in many regards. Differences include measuring the SEE cross section as a function of proton energy as opposed to LET, as well as differences in cumulative fluence and particle flux rates.

3) Proton Damage Testing

Proton damage tests were performed on biased devices with functionality and parametrics being measured either continually during irradiation (in-situ) or after step irradiations (for example, every 10 krad (Si), or every $1x10^{10}$ protons).

4) Pulsed Laser Facility Testing

The laser light used had a wavelength of 590 nm that resulted in a skin depth (depth at which the light intensity decreased to 1/e - or about 37% - of its surface intensity) of

2 microns. A pulse rate of 100 Hz was chosen. The DUT was mounted on an X-Y stage in front of a 100x lens that produced a spot size of about 1.5 microns. The X-Y stage could be moved in steps of 0.1 micron for accurate positioning of SEU sensitive regions in front of the focused beam. An illuminator together with a CCD camera and monitor were used to image the area of interest, thereby facilitating accurate positioning of the device in the beam. The pulse energy was varied with a neutral density filter and the energy was monitored by splitting off a portion of the beam and directing it at a calibrated energy meter.

5) TID Testing

TID testing was performed to MIL-STD-883 1019.5 test method. TID testing was performed at NAVSEA Crane Code 6054, using a Shepherd Model 484 Cobalt-60 tunnel irradiator. TID testing was also performed using a Co-60 source at the Goddard Space Flight Center Radiation Effects Facility (GSFC REF). The source is capable of delivering a dose rate of 0.5 Rad(Si)/s, with dosimetry being performed by an ion chamber probe.

III. TEST RESULTS OVERVIEW

Abbreviations and conventions are listed in Table IV. Abbreviations for principal investigators (PIs) and test engineers are listed in Table V. Definitions for the categories are listed in Table VI. SEE test results are summarized in Table VII. SEL test results are summarized in Table VIII. Displacement Damage results are summarized in Table IX. TID results are summarized in Table X. Unless otherwise noted, all LETs are in MeV•cm^2/mg and all cross sections are in cm^2/device. This paper is a summary of results. Complete test reports are available online at http://radhome.gsfc.nasa.gov [1].

TABLE IV: ABBREVIATIONS AND CONVENTIONS:

H = heavy ion test
P = proton test (SEE)
LET = linear energy transfer (MeV•cm^2/mg)
LET_{th} = linear energy transfer threshold (the minimum LET value for which a given effect is observed for a fluence of $1x10^7$ particles/cm^2 – in MeV•cm^2/mg)
LET_{max} = highest tested LET
LET_{eff} = effective LET
SEU = single event upset
SEL = single event latchup
SET = single event transient
SEFI = single event functional interrupt
DD = displacement damage
< = SEE observed at lowest tested LET
> = No SEE observed at highest tested LET
TID = total ionizing dose
σ = cross section (cm^2/device, unless specified as cm^2/bit)
σ_{SAT} = saturation cross section at LET_{max} (cm^2/device, unless specified as cm^2/bit)
LDC = lot date code
MEMS = Microelectromechanical System

TABLE V: LIST OF PRINCIPAL INVESTIGATORS AND TEST ENGINEERS

Abbreviation	Principal Investigator (PI) & Test Engineers
JB	John Bings
SB	Steve Buchner
MC	Marty Carts
JF	Jim Forney
JH	Jim Howard
MJ	Mike Jones
HK	Hak Kim
SK	Scott Kniffin
KL	Ken LaBel
RL	Ray Ladbury
CM	Cheryl Marshall
PM	Paul Marshall
CP	Christian Poivey
RR	Robert Reed
AS	Anthony Sanders
CS	Christina Seidleck
JT	Jeff Titus

TABLE VI: LIST OF CATEGORIES

Category	Implications
1	Recommended for usage in all NASA/GSFC spaceflight applications
2	Recommended for usage in NASA/GSFC spaceflight applications, but may require mitigation techniques
3	Recommended for usage in some NASA/GSFC spaceflight applications, but requires extensive mitigation techniques or hard failure recovery mode
4	Not recommended for usage in any NASA/GSFC spaceflight applications

TABLE VII: SUMMARY OF SEE TEST RESULTS

Part Number	Function	LDC	Manufacturer	Particle: (Facility;Date)P.I.	Testing Preformed	Summary of Results	Cat.
Op Amps & Analog Comparators:							
LM124	Op Amp		National Semiconductors	H: (BNL01DEC) CP/SK Laser: (NRL01MAY) KL/CP/JH	SET	H: (BNL01DEC) Data analysis in progress Laser: (NRL01MAY) Various transient shapes were observed depending on the application and bias conditions	2
LM119	Voltage comparator		NSC	H: (BNL01DEC) SB	SET	LET = 11.44, 24.21, and 59.87	2

TABLE VII (CONT.): SUMMARY OF SEE TEST RESULTS

Part Number	Function	LDC	Manufacturer	Particle: (Facility;Date)P.I.	Testing Preformed	Summary of Results	Cat.
Programmable Devices:							
PALCE22V10	Programmable logic device	0134	Cypress	H: (BNL02MAR) SK	SEL/SET	SEFI at LET=7.9, one non-destructive SEL at same (SEFI renders this device non-useable by the project)	3
ATF22V10B	Programmable logic device	0127	Atmel	H: (BNL02MAR) SK	SEL/SET	No SEL up to LET of 84.39 some SETs, timing and output SETs are max s of $1x10^{-6}$, the Hi-Low mismatch max s is $1.5x10^{-5}$	2
GAL22V10/883	Programmable logic device	0043	Lattice	H: (BNL02MAR) SK	SEL/SET	SEL at LET = 26.55 as well as mismatch errors	3
AN10E40	Analog FPGA	0051	Anadigm	H: (BNL02MAR) AS/SK	SEL/SET	SET LET_{th} < 11.44, SEL LET_{th} = 19.9	4
Power Devices:							
MDI3051RES05ZF	DC/DC Conv.	0130	MDI	H: (TAMU01OCT) JH	SET/SEGR/SEB	No SET's observed to an LET of 60. Destructive event observed at an LET of 37 under high load	3
MDI3051RED12ZF	DC/DC Conv.	0132	MDI	H: (TAMU01OCT) JH	SET/SEGR/SEB	No SET's observed to an LET of 60. Destructive event observed at an LET of 60 under modeate load	3
MDI3051RED15ZF	DC/DC Conv.	0132	MDI	H: (TAMU01OCT) JH	SET/SEGR/SEB	No SET's observed to an LET of 60. Destructive event observed at an LET of 60 under high load	3
LM2651	Switching Regulator		National Semiconductor	H: (BNL02MAR) CP	SEL/SET	LETth failure~25; Xsat failure ~2.5 X 10^{-5} LETth SET~5; Xsat SET=$1.5X10^{-4}$ destructive failures observed	3/4
MSK5042	Switching Regulator	0204	MS Kennedy	H: (BNL02MAR) CP/SB	SEL/SET	Functional failures (SEB) at 37	3/4
LP3470	Voltage Supervisor	0036	National Semiconductor	H: (BNL02MAR) CP/SK	SEL/SET	no SEL up to 27 (maximum tested LET) SET LETth=1.5 SET Xsec= $8X10^{-5}$ at 8 $MeVcm^2/mg$	4
ADCs and DACs::							
AD7714	24 bits ADC		Analog Devices	H: (BNL01DEC) CP/SK (BNL02MAR) SB	SEE	SEL at a LET of 24 (No SEL at LET of 16). Cross section SEL=3E-4 at a LET of 48 SEU LETth~4; SEUcross section=$5.6x10^{-5}$ at a LET of 15	3
AD7821	8 bits ADC, 1 MSPS	0034	Analog Devices	H: (TAMU01JUL) CP	SEE	No SEL up to a LET of 80 SEU LETth~4; Xsat=$4x10^{-4}$	2
AD9223	12 bits ADC, 3 MSPS	0015	Analog Devices	H: (TAMU01JUL) CP	SEE	Sensitive to SEL at a LET of 20; no SEL at a LET of 11.4; SEU LETth~ 11	2
LTC1272	12 bits ADC, 250 kHz	0018	Linear Technology	H: (TAMU01JUL) CP	SEE	SEL LETth~5; SEL cross section=$1x10^{-4}$ at a LET of 20; SEU LETth=4	4
LTC1657	ADC 16 bits	0105	Linear Technology	H: (BNL02MAR) CP	SEE	LETth SEL~14 Xsection SEL=6.3E-5cm2 at a LET of 37 LETth SEU/SET~4 Xsection SEU/SET=1.2E-3 at a LET of 37	3
ADC1175	DAC 8 bits 20 MHz	1317	National Semiconductor	H: (BNL02MAR) CP; (TAMU02MAR) RR/RL/JH	SEL(BNL)/SEU (TAMU)	LETth SEL~23; Xsection SEL=4.6E-4cm2 at a LET of 118	3

TABLE VII (CONT.): SUMMARY OF SEE TEST RESULTS

Part Number	Function	LDC	Manuf.	Particle: (Facility)P.I.	Testing Preformed	Summary of Results	Cat.
Communication Devices:							
TSB12LV26PZT	Link 1394 FireWire OHCI Chipset	045T	TI	H: (BNL01AUG) PM; (TAMU01OCT) SB/PM/KL P: (TRIUMF01JUL) SB/CS	SEU; SEFI; SEL	Many types of non-destructive SEFI were observed P: σ = 1.48E-10	3
TSB41AB3PFP	Physical 1394 FireWire OHCI Chipset	4RTT	TI	H: (BNL01AUG) PM; (TAMU01OCT) SB/PM/KL P: (TRIUMF01JUL) SB/CS	SEU; SEFI; SEL	Many types of non-destructive SEFI were observed P: σ = 5.98E-11	3
CS4210VJG	Link 1394 FireWire OHCI Chipset		NSC	H: (BNL01AUG) PM P: (TRIUMF01JUL) SB/CS	SEU; SEFI; SEL	Many types of non-destructive SEFI were observed P: σ = 2.56E-10	4
CS4103VHG	Physical 1394 FireWire OHCI Chipset		NSC	H: (BNL01AUG) PM P: (TRIUMF01JUL) SB/CS	SEU; SEFI; SEL	Many types of non-destructive SEFI were observed P: σ = 1.46E-10	4
M3-SW16-8S	16 Port Myrinet Crossbar Switch MYRI2K	84312 87091	Myricom	P: (CNL01OCT) JH/MC	SEE; P:TID	No Latchups observed. Functional Interrupts and data loss was observed at the system level.	3
Lanai9	Myrinet NIC Protocol Processor MYRI2K	0118	Myricom	P: (CNL01OCT) JH/MC	SEE	No Latchups observed. Functional Interrupts and data loss was observed at the system level.	3
SerDeSer	Myrinet Serializer-Deserializer MYRI2K	0123	Myricom	P: (CNL01OCT) JH/MC	SEE	No Latchups observed. Functional Interrupts and data loss was observed at the system level.	3
PCIDMA	Myrinet PCI to DMA	0126	Myricom	P: (CNL01OCT) JH/MC	SEE	No Latchups observed. Functional Interrupts and data loss was observed at the system level.	3
VCS7146RH	Myrinet Transceiver MYRI2K		Vitesse	P: (CNL01OCT) JH/MC	SEE	No Latchups observed. Functional Interrupts and data loss was observed at the system level.	3
K7N803601M	SRAM (in Myrinet System)		Samsung	P: (CNL01OCT) JH/MC	SEE	No Latchups observed. Functional Interrupts and data loss was observed at the system level.	3
AD8151	Crossbar Switch		Analog Devices	P: (CNL02JAN) SB/PM/RR H: (TAMU02MAR) RR/RL/JH	SEE (also see DD and TID tables) P: DD/TID	Peak in the BER at a LET of 7; No SEL to 60	3

TABLE VII (CONT.): SUMMARY OF SEE TEST RESULTS

Part Number	Function	LDC	Manuf.	Particle: (Facility)P.I.	Testing Preformed	Summary of Results	Cat.
Miscellaneous:							
LSP2916	High Voltage Drives (MEMS)	0134? 0127? 0043?	Agere Systems	H: (BNL01DEC) SK	SEE	Devices exhibited destructive SEL at an LET of 26, partial to complete bond wire vaporization was the result	3
Photobit APS	APS		Photobit	H: (TAMU01MAR) CM/PM/RR	SEU/SEL	No SEL to LET of 106, SETs observed	2/3
Test Sample	5HP SiGe Prescaler		IBM	P: (CNL01MAR) RR; (TAMU01JUL)TBD (TAMU01MAR) TBD	SEU	Bit upsets at 63MeV protons	2/3
PE9301	SOS Prescaler		Peregrine	P: (CNL01MAR) RR; (TAMU01JUL)TBD (TAMU01MAR) TBD	SEU	Bit upsets at 63MeV protons	2/3
MTX8501	Transmitter		Emcore	P: (CNL02FEB) SB/PM/RR	SET	No SETs observed at 63MeV protons	1
MRX8501	Receiver		Emcore	P: (CNL02FEB) SB/PM/RR	SET	SETs observed with angular effects on photodetector	2
Processor Boards:							
Pentium PIII 1000 MHz	Processor		Intel	P: (IU01MAY) JH (IU02FEB?) JH H: (TAMU01MAR & OCT) JH/KL	SEL; SEU; SEFI	No SEL up to 5.0 x 10^{10} protons/cm^2 and LET ~15 SEU and SEFIs observed with protons and with HI at LET $\leq$0.7	3
Pentium PIII 933 MHz	Processor		Intel	P: (IU01MAY) JH (IU02FEB?) JH H: (TAMU01MAR & OCT) JH/KL	SEL; SEU; SEFI	No SEL up to 5.0 x 10^{10} protons/cm^2 and LET ~15 SEU and SEFIs observed with protons and with HI at LET $\leq$0.7	3
Pentium PIII 850 MHz	Processor		Intel	P: (IU01MAY) JH (IU02FEB?) JH	SEL; SEU; SEFI	No SEL up to 5.0 x 10^{10} protons/cm^2 and LET ~15	3
Pentium PIII 800 MHz	Processor		Intel	H: (TAMU01MAR) JH/KL	SEFI	SEU and SEFIs observed with protons and with HI at LET $\leq$0.7	3

TABLE VIII: SUMMARY OF SEL TEST RESULTS

Part Number	Function	LDC	Manuf.	Particle: (Facility)P.I.	Testing Preformed	Summary of Results	Cat.
ADCs:							
LTC1604	16 bits ADC, 333ksps; SSOP 36 pin		Linear Technology	H: (TAMU01JUL) CP (TAMU01AUG) CP	SEL	No SEL up to a LET of 65 MeVcm2/mg	2
LTC1605	16 bits ADC, 100 ksps; SSOP 28 pin	9914	Linear Technology	H: (TAMU01OCT) CP/JH	SEL	SEL at a LET of 53 MeVcm2/mg SEL σ >1E-2cm2 Recovers normal functionality after power cycle	3
LTC1608	16 bits ADC	0120	Linear Technology	H: (BNL02MAR) CP/SK	SEL	SEL at 85 MeVcm2/mg Xsection=2.4E-7 at a LET of 94 MeVcm2/mg	3

TABLE VIII (CONT.): SUMMARY OF SEL TEST RESULTS

Part Number	Function	LDC	Manuf.	Particle: (Facility)P.I.	Testing Preformed	Summary of Results	Cat.
Miscellaneous:							
ADG452	Analog Switch; SOIC 16	0129	Analog Devices	H: (BNL01DEC) CP/SK	SEL	No SEL up to a LET of 82 MeVcm2/mg	1
ICL7662	Voltage converter; CAN 8	0135	Intersil	H: (BNL01DEC) CP/SK	SEL	No SEL up to a LET of 82 MeVcm2/mg	1
XA1	ASIC		AMS CMOS	H: (TAMU01MAR) RL/SK	SEL		4
PCA80C522	Processor	9707	Phillips	H: (BNL01AUG) JH/KL (BNL01DEC) JH	SEL	SEL LET_{th} >3, σ_{sat}>$3x10^{-3}$. Latchup is not destructive unless part is left latched for > 30 seconds [4]	3

TABLE IX: SUMMARY OF DISPLACEMENT DAMAGE TEST RESULTS

Part Number	Function	LDC	Manufacturer	Particle: (Facility)P.I.	Testing Preformed	Summary of Results
Misc:						
BAE CCD486	ACS 4kx4k WFC CCD Detector	S/N 3188	British Aerospace	P: (CNL01MAR) MJ/RR/PM	Displacement Damage	Power law parallel CTE behavior; Evidence of mini-channel signature in serial CTE
TIL25	GaAs LED		Texas Instruments	P: (CNL01MAY) SK/JH/RR	Displacement Damage	Significant degradation at total fluence of $2.56x10^{10}p/cm^2$
TIL601	Opto Transistor		Texas Instruments	P: (CNL01MAY) SK/JH/RR	Displacement Damage	Significant degradation at total fluence of $6.4x10^{10}p/cm^2$
4N49	Opto	9803 and 9818	MII	P: (CNL01MAY) SK/RR	Displacement Damage	Greater than acceptable V_{CE} values at $1x10^{11}p/cm^2$

TABLE X: SUMMARY OF TID TEST RESULTS

Part Number	Function	LDC	Manufacturer	(Facility;Date)P.I.	Testing Preformed	Summary of Results	Cat.
ADCs:							
AD7714	24 bits ADC	0041	Analog Devices	(NAVSEA 02FEB) JB/CP	TID	Non-functional between 10Krad(Si) and 20Krad(Si) Degradation between 7.5 Krad(Si) and 20Krad(Si) No degradation in integral nonlinearity up to 10Krad(Si)	2
LTC1272	12 bits ADC, 250 kHz	0018	Linear Technologies	(NAVSEA 01DEC) JB/CP	TID	Parametric failures were observed at 5krad(Si) on all devices	2
AD6640	12 bit, 65 MHz monolithic ADC	9951	Analog Devices	(NAVSEA 01NOV) JB/JH	TID	No significant degradation to 100Krads(Si)	1
Power MOSFETs:							
FDN361AN	30V N channel MOSFET; Super SOT-3	0133	Fairchild	(NAVSEA 01DEC) JT/CP	TID	Within specification up to 20 krad (Vth)	2

TABLE X (CONT.): SUMMARY OF TID TEST RESULTS

Part Number	Function	LDC	Manufacturer	(Facility;Date)P.I.	Testing Preformed	Summary of Results	Cat.
Power MOSFETs (Cont.):							
NDS352A	30V P channel MOSFET; Super SOT-3	0053	Fairchild	(NAVSEA 01DEC) JT/CP	TID	All parameters within specification at 50 krad	2
IRLML2803A	30V N channel MOSFET; Micro 3	0103	International Rectifier	(NAVSEA 01DEC) JT/CP	TID	Within specification up to 35 krad (Vth)	2
IRLML5103A	30V P channel MOSFET; Micro 3	0034	International Rectifier	(NAVSEA 01DEC) JT/CP	TID	Within specification up to 35 krad (Rdson)	2
Processor Boards:							
Pentium III 550; 650; 700; 800; 850; 933 MHz and 1 GHz	Processor		Intel	(GSFC 02JAN) JH	TID	Biased and operating levels are 500-800 krads(Si); Unbiased failure levels >3 Grads(Si)	1
Misc:							
2N5114	30V P channel JFET; TO18	9518	New England	(NAVSEA; 02JAN) JT/CP	TID	IDSS and IGSS exceeded their specification limit at 50 krad(Si)	2
AD8151	Crossbar Switch		Analog Devices	P: (CNL02JAN) SB/PM/RR H: (TAMU02MAR) RR/RL/JH	TID? Ask CP	Shows no changes in supply current up to a TID of 14 krad(Si) Degradation in performance at ~70 krad(Si); current increased with dose up to 168 krad(Si) NOTE: Functionality testing only - Not full TID parametric evaluation	3

IV. SEE Test Results and Discussion

As in our past workshop compendia of GSFC test results, each DUT will have an individual section describing in further detail, test method, SEE or degradation conditions/parameters, test results, and graphs of data.

A. Op Amps & Analog Comparators:

1) LM124

Four different applications have been investigated for the LM124: voltage comparator, non inverting gain (x101), non inverting gain (x11), and voltage follower. Different power supply and input bias conditions have been investigated. (see test report and NSREC2001 paper for more details)

The output of the Device Under Test (DUT) is monitored with a digital oscilloscope. As soon as the DUT output exceeds a given trigger level (generally 500 mV), an SET is counted and the complete SET transient data is stored on a computer for future analysis.

Heavy ion testing was performaed at the TEXAS A&M cyclotron. The LM124 results showed a large variety of transient waveforms and a significant impact of the power supply voltage.

The LM124 exhibits a very low sensitivity when it is used as a voltage comparator. The LM124 exhibits a higher SET sensitivity when it is used as a non-inverting gain amplifier or a voltage follower. Fig. 1 shows the worst case SET cross section curve for the non-inverting gain of 11 application. The LET threshold is lower than 2.86 $MeVcm^2/mg$ and the maximum cross section is about $3x10^{-5}$ cm^2/amplifier.

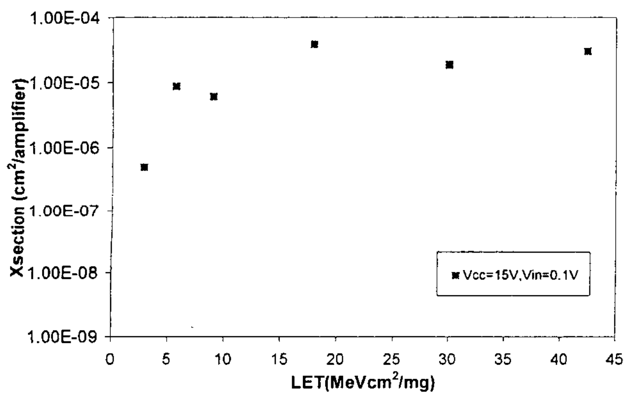

Fig. 1: LM124 SET cross section curve.

These worst case results have been obtained with a +/-15V power supply voltage for both input voltages investigated. The worst case cross-sections for the non inverting gain of 101 and the voltage follower applications are similar for the +/-15V power supply voltage, but we see an effect of the input voltage near the LET threshold. Near the threshold, the lower input voltages give the higher SET sensitivities.

When the power supply voltage is +5/0V, the SET sensitivity is significantly lower for high input voltages. In these conditions, no event has been observed at the LET of 9 $MeVcm^2/mg$ and only a few events have been observed at the LET of 30 $MeVcm^2/mg$.

Three different types of transients have been observed. First, large bipolar transients that are predominant especially at low LET. The transient's negative going component characteristics are very dependant on the application (higher is the gain lower is the amplitude and duration and the power supply voltage). The overall transient characteristics vary with the LET. Second, long duration positive going transients that only appear at high LET and could represent up to 35% of the total number of transients. Finally, small positive going transients that are marginal at low LET and could represent up to 25% of the total number of transients at high LET.

An example of a large bipolar transient is shown in Fig. 2. The transient's positive going component goes up to the +Vcc rail and has a 1.5 μs FWMH. The worst case amplitude of long duration transients is 2V and their maximum FWMH is larger than 10 μs. The worst case amplitude of a small transient is 2V. The worst case FWMH is 600 ns. For more details see "Development of a Test Methodology for Single Event Transients (SET) in Linear Devices". [NRL01MAY_LM124.pdf] [nsrec01_ph2]

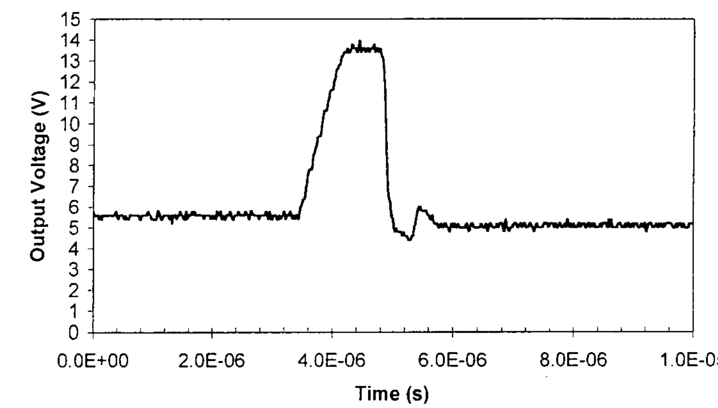

Fig. 2. LM124, Non inverting gain x101 application, typical large bipolar transient, LET = 2.86 MeVcm2/mg, Vcc = +/- 15V, V+ = 0.05V.

2) LM119

LM119 (National Semiconductor). Single-Event-Testing (SET) was performed on the LM119 voltage comparator using heavy ions at Brookhaven National Laboratory. The dependence of the SET cross-section on supply voltage, differential input voltage and output load were measured. The LM119 was tested under the following conditions:

- Vdd = 5V, 10V, and 15V
- Δ V = +4.5V, +2.5V, +0.12V, -0.2, and –4.5V
- R = 1.7 KΩ and 0.17 KΩ
- Angles = 0° and 60°
- LET = 11.44 $MeV.cm^2/mg$, 24.21$MeV.cm^2/mg$ and 59.87 $MeV.cm^2/mg$

The cross-section for positive differential input voltage was an order of magnitude smaller than for negative differential input voltage, confirming the results of pulsed laser testing. Fig. 3 shows the cross section as a function of LET for both positive and negative values of ΔV. Fig. 3 also shows that the cross-section increases at higher positive values for ΔV but does not do so for negative values of ΔV. Fig. 4 shows that the cross-section increases with increasing supply voltage. Also there was no dependence of the cross-section on the output load, which was varied by a factor of 10X. [B122101_paper_ lm119.pdf] [B122101_lm119.pdf]

LM119

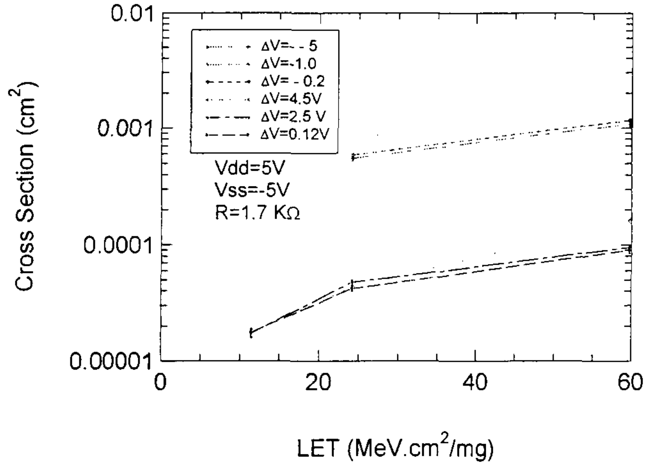

Fig. 3. SET cross-section as a function of ion LET for the LM119 voltage comparator for positive and negative differential input voltages. The cross-section is an order of magnitude greater for negative differential input voltage than for positive differential input voltages. Also, at an effective LET of 60 MeV.cm^2/mg, the cross-section for ΔV = 4.5 V is greater than at 2.5 V.

LM119

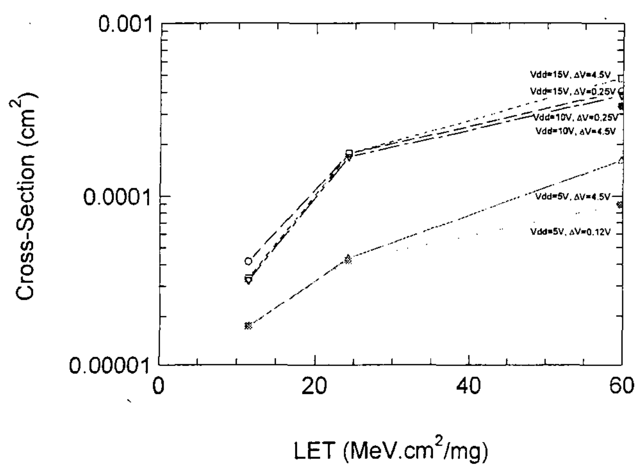

Fig. 4. SET cross-section as a function of ion LET for the LM119 voltage comparator for different combinations of supply voltage (V_{dd}) and differential input voltage (Δ V). The general trend is that the cross-section is larger for larger supply voltages.

B. *Programmable Devices:*

1) *PALCE22V10*

Cypress PALCE22V10. The DUTs showed SEFI and one non-destructive SEL at an LET of 7.9 MeV•cm^2/mg (Si-28 at normal incidence). Typically, the SEFI occurred simultaneously with ~110-130 errors from Outputs 1-6 while the counter monitoring the High and Low rail of the device counted literally every clock cycle as one of the rails had failed. Each time the device recovered after a reset. Nominal current was 76mA; during one run, DUT C2 latched and the power supply current went to 110mA and recovered after a reset. A summary of all effects is given below in Table 11. [B030402_22V10.pdf]

2) *ATF22V10B*

Atmel ATF22V10B. The DUTs showed no SEL up to an LET of 84.39 MeV•cm^2/mg (I-127 at 45° from normal incidence). One DUT was also tested at an LET of 84.1 MeV•cm^2/mg (Au-197 at normal incidence) with no SEL. There were a few SET mismatch errors, with the cross section tending to increase slightly with increasing LET. The mismatch threshold LET was 13.21 MeV•cm^2/mg (Cl-35 at 30° from normal incidence). Additionally, the software can detect timing errors when they occur separately from other mismatch errors in Outputs 1-6. These timing errors were detected in several runs with timing error threshold LET of 23.02 MeV•cm^2/mg (Cl-35 at 45° from normal incidence). The High/Low comparator also saw an increasing number of SETs with increasing LET, with a comparator threshold LET of 11.44 MeV•cm^2/mg (Cl-35 at normal incidence). A summary of all effects is given below in Table 11. [B030402_22V10.pdf]

3) *GAL22V10/883*

Lattice GAL22V10/883. The DUTs showed a non-destructive SEL with an LET threshold of 26.55 MeV•cm^2/mg (Ni-58 at normal incidence). Typical I_{CC} was ~20mA and the SEL took the current to 99-110mA. These events also led to the High/Low rail counter monitor to count all clock cycles as in the case of the Cypress parts. There were very few SET mismatch errors, typically one or two per run. The threshold for mismatch errors was at an LET of 22.88 MeV•cm^2/mg (Cl-35 at 60° from normal incidence). Additionally, timing errors were detected in four runs with the same onset as that of the mismatch errors. A summary of all effects is given below in Table 11. [B030402_22V10.pdf]

TABLE 11: SUMMARY OF SEE FOR 22V10 DEVICES. ALL NUMBERS GIVEN ARE IN MEV•CM^2/MG.

Manufacturer	Mismatch SET	SEFI	SEL	High/Low SETs	Timing Error SETs
Cypress PALCE22V10	Occurred with SEFI	LET_{th} = 7.9	One at LET of 7.9	Continuous errors with SEFIs or SEL	Some occurred with SEFIs
Atmel ATF22V10B	σ_{th} = 13.21	None detected	None up to LET of 84.39	LET_{th} = 11.44	LET_{th} = 23.02
Lattice GAL22V10/883	σ_{th} = 22.88	None detected	LET_{th} = 26.55	Onset at LET of 11.44 but continuous errors with SELs	LET_{th} = 22.88

4) *AN10E40*

Heavy ion testing was performed at Brookhaven National Laboratory's Single Event Upset Test Facility on the AN10E40 Field Programmable Analog Array (FPAA) manufactured by Anadigm. The test setup was comprised of an Anadigm evaluation board that housed the DUT. From the evaluation board, a configuration of a gain stage of 5 was programmed into the DUT. A function generator provided a 1kHz signal, riding on a 2.5V rail, to the input and an output of a gain of 5 was captured using a digitizing oscilloscope. A counter built into the scope was used to count the number of triggers (SETs). A power supply provided input voltage to the DUTs.

Two devices were tested. Both DUTs experienced SETs and loss-of-configuration errors at an LET of 11.44 MeV• cm^2/mg. DUT 2 was experiencing SETs with the beam off after approximately 10 krads(Si) total dose. DUT 3 also experienced non-destructive SEL at a threshold LET of 19.9MeV• cm^2/mg (Cl-35 at 55°). Following these SELs, the current to the test board increased by a factor of two. The device reset after power cycling. For the configuration σ_{SET} = ~$4x10^{-6}$ cm^2. [B030402_AN10E40.pdf]

C. Power Devices:

1) MDI3051RES05ZF, MDI3051RED12ZF, and MDI3051RED15ZF

The Modular Devices, Inc. MDI3051RES05ZF, MDI3051RED12ZF and MDI3051RED15ZF DC/DC Converters were monitored for transient interruptions in the output signal and for destructive events induced by exposing it to a heavy ion beam at the Texas A&M University Cyclotron Single Event Effects Test Facility. These tests were performed at a flux of $4x10^4$ to $6x10^4$ particles/cm^2/s. All DC/DC converters tested were de-lidded and the active device area divided into three circular regions. Region number 1 is the power MOSFET, Region #2 contained the linear devices at the device output and Region #3 is a linear device near the MOSFET.

The test hardware for this testing was a digitizing oscilloscope, programmable power supplies and an electronic load. The programmable power supplies were used as an input to the DC/DC converter, allowing remote control of the input voltage. The output from the devices was swept across the high impedance input of the digital scope and into an electronic load that maintained the device loading constant via a constant current mode on the output of the device. Any transients that appeared on the output pins of the devices were captured and saved to a file. The definition of a destructive event is an event that causes the output of the device to change to a value outside the specifications and that power cycling the device does not lead to a recovery of functionality.

Due to the high power nature of this devices, special attention needed to be placed on the temperature control of the device. The device was mounted to a copper plate via a thremasil pad (electrically non-conductive, thermally highly conductive). The temperature of the device was monitored. Since the device sits in air in the TAMU facility, no forced cooling through the tubing was required. During the entire testing, the temperature remained between 20 and 25 °C.

The MDI3051RES05ZF was tested using Energy Degraded Kr 37, and Energy Degraded Xe 60. The sample size of the testing was limited to one device. The device tested had a serial number of 2006, and a Lot Date Code of 0130.For all of the conditions and all regions, no single event transients were observed at the output voltage port. However, the device did experience a destructive event when the MOSFET was exposed under the 126 volt, 75% loading condition and an LET of 37 (Kr). That event resulted in the output dropping to zero volts and a loss of functionality that was not recovered after a power cycle. Prior to that failure, the device successfully ran through approximately 10^7 cm^{-2} ions at the other four test conditions for both an LET of 28.4 and 37 MeV•cm^2/mg. It should be noted that no load condition greater than 50% was run at an LET less than 37. This could mean that for high load conditions, the failure might be seen at much lower LETs. The cross section for this one failure was approximately 5 x 10^{-7} cm^2. However, due to the sample size being only one device there could be substantial variation in this number.

The MDI3051RED12ZF was tested using Kr 28.4, Energy Degraded Kr 37, and Energy Degraded Xe 60. The sample size of the testing was limited to one device. The device tested had a serial number of 2019, and a Lot Date Code of 0132. The MDI3051RED12ZF was tested under bias conditions of 120 and 126 volts at a loading of approximately 9.37 (25%), 18.72 (50%) and 28.1 (75%) watts. The DC/DC converter was de-lidded and the active device area divided into three circular regions. Region number 1 is the power MOSFET, Region #2 contained the linear devices at the device output and Region #3 is a linear device near the MOSFET.

For all of the conditions and all regions, no single event transients were observed at the output voltage port. However, the device did experience a destructive event when the MOSFET was exposed under the 120 volt, 50% loading condition and an LET of 60. That event resulted in the output dropping to zero volts and a loss of functionality that was not recovered after a power cycle. Prior to that failure, the device successfully ran through approximately 10^7 cm^{-2} ions at the other test conditions including:

- 75% loading at 120 volts at an LET of 28.4
- 75% loading at 126 volts at an LET of 28.4
- 50% loading at 120 volts at an LET of 37
- 25% loading at 120 volts at an LET of 60

The cross section for this one failure was approximately 2.5 x 10^{-6} cm^2. However, due to the sample size being only one device there could be substantial variation in this number.

The MDI3051RED15ZF was tested using Energy Degraded Kr 37, and Energy Degraded Xe 60. The sample size of the testing was limited to one device. The device tested had a serial number of 2001, and a Lot Date Code of 0132. The MDI3051RED15ZF was tested under bias conditions of 120 volts at a loading of approximately 9.38 (25%) and 28.13 (75%) watts and 126 volts at a loading of approximately 9.38 (25%), 18.75 (50%) and 28.13 (75%) watts.

For all of the conditions and all regions, no single event transients were observed at the output voltage port. However, the device did experience a destructive event when the MOSFET was exposed under the 120 volt, 75% loading condition and an LET of 60. That event resulted in the output dropping to zero volts and a loss of functionality that was not recovered after a power cycle. Prior to that failure, the device successfully ran through approximately 10^7 cm^{-2} ions at the other test conditions including:

75% loading at 120 volts at an LET of 37
75% loading at 126 volts at an LET of 37
25% loading at 120 volts at an LET of 60

The cross section for this one failure was approximately 2.6 x 10^{-6} cm^2. However, due to the sample size being only one device there could be substantial variation in this number. [T100115_MDI05.pdf] [T100115_MDI12.pdf] [T100115_MDI15.pdf]

2) LM2651

The monolithic switching regulator LM2651 from National semiconductor was tested at BNL using ions with an effective LET ranging from 11.4 MeVcm2/mg (Chlorine at 0 degree) to 37.5 MeVcm2/mg (Bromine at 0 degree). Three different load conditions have been tested (no load, 40% and 60% of maximum load). The transient LET threshold is about 5 MeVcm^2/mg. The transient cross section measured at the maximum LET is about 1.5x10^{-4} cm^2/device. The three parts experienced destructive failures. The highest load appears to be the worst case configuration for destructive failures. No failure was observed up to a LET of 26 MeVcm^2/mg and a fluence of 1E7 ions/cm^2 for all load conditions. The first failure occurred at a LET of 37.4 MeVcm^2/mg for the maximum load condition. The failure cross section at the maximum tested LET is about 2.5x10^{-6} cm^2/device. On two parts (SN1 and SN2) the output voltage is at 0 V after the failure. On SN3, the output voltage is equal to +Vin (10V) after the failure. On SN1 and SN3 the failure occurred at the bonding of one of the device output power MOSFET as shown in Figure 5. As shown in the picture the bonding has vaporized. No apparent failure was observed on the MOSFET. [B030302_LM2651.pdf]

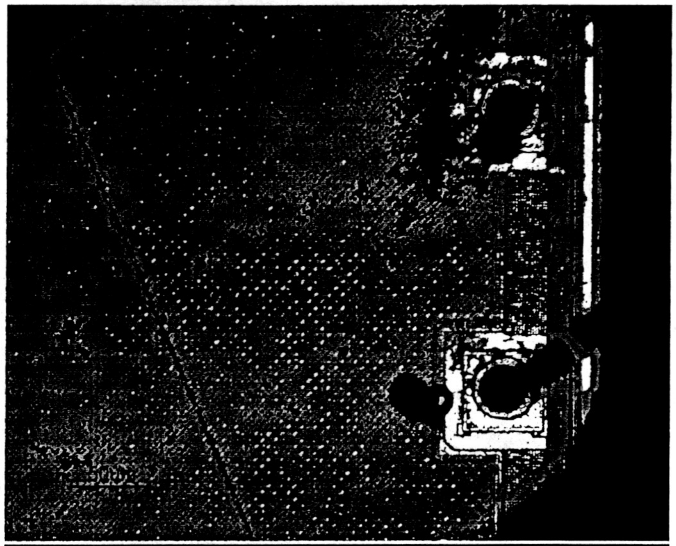

Fig. 5: picture of the vaporized bonding at the output MOSFET of the LM2651.

3) MSK5042

The MSK5042 is a hybrid switching regulator. This part uses four different SEE sensitive device types: one PWM controller MAX797 from MAXIM, two 55V N channel power MOSFET IRLC034N from International Rectifier, one voltage reference REF43 from Analog Devices, and one operational amplifier AD822 from Analog Devices. The part has been biased with the 30V maximum input voltage. The output voltage has been adjusted to 2.5V. This part has been tested for SET and SEL at BNL using ions with and effective LET ranging from 11.4 MeVcm^2/mg (Chlorine at 0 degree) to 84 MeVcm^2/mg (Iodine at 45 degrees). The PWM controller has been irradiated alone, and the four other sensitive devices have been irradiated together. Figure 6 shows the two different irradiated areas. A very low transient sensitivity has been observed for both areas. When the MOSFET and linear area was irradiated, two failures were observed, one at the LET of 59 MeVcm^2/mg and the other at the LET of 37 MeVcm^2/mg. These failure are attributed to Single Event Burnout on the power MOSFETs. Figure 7 shows the failure on one power MOSFET. [B030302_MSK5042.pdf]

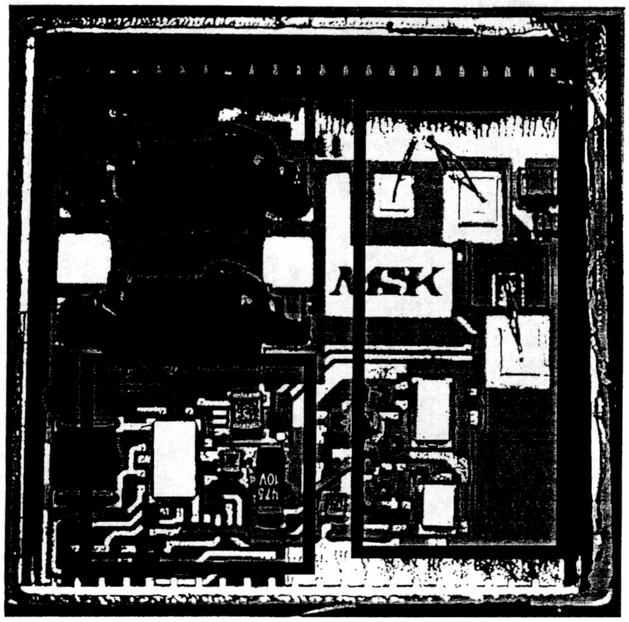

Fig. 6: Irradiated area, first area on the left includes the MAX797, second area includes the power MOSFETs, the voltage reference, and the operational amplifier.

Fig. 7: burnout on a power MOSFET.

4) LP3470

The LP3470 power on reset circuit from National Semiconductors was tested at BNL using ions with an effective LET ranging from 1.4 MeVcm^2/mg (Carbon at 0 degree) to 27 MeVcm^2/mg (Ni at 0 degree). During testing the device reset output was monitored by a scope. As soon as this output deviates from more than 2V from the nominal value, an error is counted. The device is extremely sensitive, with 1 active reset at the lowest LET for a fluence of 1E7 ions/cm^2. Then the cross section increases very rapidly to about 8x10^{-5} cm^2/device at a LET of 2.5 MeVcm^2/mg (Oxygen at 0 degree). Above a LET of 11 MeVcm^2/mg (Chlorine at 0 degree), the reset output stays continuously activated. [B030302_LP3470.pdf]

D. ADCs and DACs:

1) AD7714

The AD7714 is 500 µA, 100 kHz, 24 bits signal conditioning ADC. The parts features three differential analog inputs (which can also be configured as five pseudo-differential analog inputs) as well as a differential reference input. The AD7714 thus performs all signal conditioning and conversion for a system consisting of up to 5 channels. The digital data is available via a serial interface. This serial interface is also used to configure the ADC gain settings, signal polarity and channel selection.

The AD7714 evaluation board has been used for the SEE testing. A program has been written that allow the part configuration, the acquisition of the serial data during the conversion and the monitoring of the conversion errors. As the part include a lot of configuration registers and upsets in these registers could affect the part functionality, a check for Single Event Functional Interrupts (SEFI) has been performed. As soon as 10 successive converted words are in error, we assumed a SEFI and the part was reconfigured. The device supply current was also monitored during the irradiation. As soon as this current reached a limit of 50 mA, the power supply was shutdown. A static 1V input voltage has been applied during the irradiation (for a full scale signal of 2.5V). With this set-up we have been able to test the 16 most significant bits out of the 24 bits.

The Figure 8 shows the SEU and SEL cross-section curves. Due to the high SEL sensitivity, it has not been possible to perform a SEU characterization for LET above 16 MeVcm2/mg. The SEU LET threshold is about 3 MeVcm^2/mg and the device SEU cross section is about 6x10^{-5} cm2 at the LET of 16 MeVcm^2/mg. Some SEFI have been observed during the experiments. Most of error are multiple errors within a corrected word, and the Most Significant Bits (MSBs) are as sensitive as the Least Significant Bit (LSB) that has been tested.The SEL LET threshold is about 16 MeVcm^2/mg (no SEL event was observed at a LET of 15 MeVcm^2/mg up to a fluence of 1E7 ions/cm^2), the device SEL cross section is about 3x10^{-4} cm^2 at the LET of 50 MeVcm^2/mg. The peak latch-up current is between 40 and 60 mA (the nominal power supply current is about 0.8 mA). Figure 9 shows a typical Latch-up current waveform.

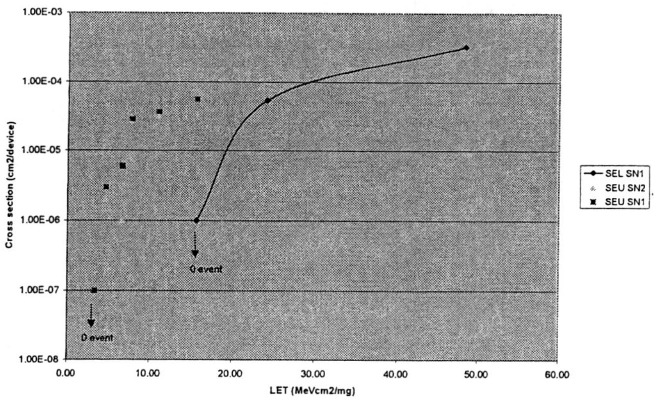

Fig. 8: AD7714, SEU and SEL cross section

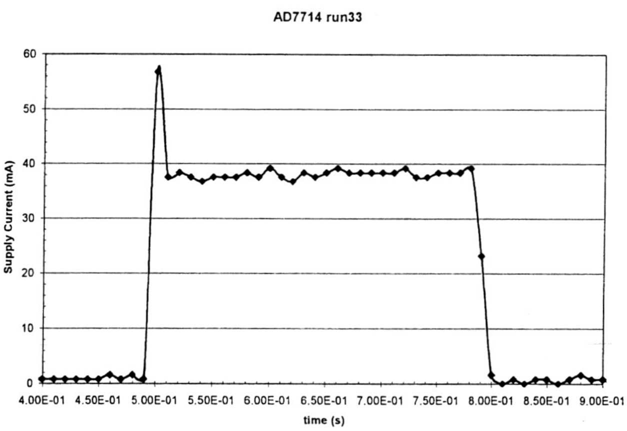

Fig. 9: Typical Latchup current waveform for the AD7714.

2) AD7821

The 8 bits ADC AD7821 from Analog Devices was tested for SEU and SEL at TAMU using ions covering a LET range from 1.8 MeVcm^2/mg (Ne at 0 degree) to 80 MeVcm^2/mg (Xe at 60 degree). The test method used is the golden chip. The same input signal is sent to the Device Under Test (DUT) and a reference device that is not irradiated. The outputs of the two devices are compared. The errors are counted and recorded. Static input signals have been applied and only the 7 MSB have been tested.

No SEL events were observed for up to the maximum tested LET and a fluence of 6E6 ions/cm^2.

The SEU LET threshold of the 4 Most Significant Bits (MSBs) and the 3 Least Significant Bits (LSBs) is the same, but the maximum SEU cross section of the MSBs is significantly more important than the sensitivity of the LSBs (ratio >2). The total SEU cross section curve for the 7 tested bits is shown in Figure 10. [T080101_ADC.pdf]

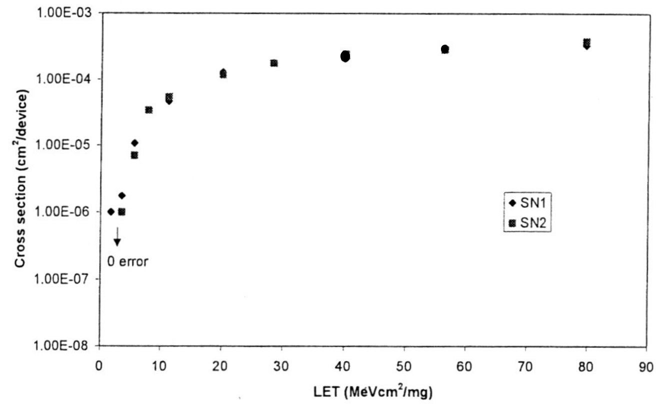

Fig 10: AD7821 SEU cross section curve

3) AD9223

The 12 bits ADC AD9223 from Analog Devices was tested for SEU and SEL at TAMU using ions covering a LET range from 1.8 MeVcm^2/mg (Ne at 0 degree) to 40 MeVcm^2/mg (Xe at 0 degree). The test method used is the golden chip. The same input signal is sent to the Device Under Test (DUT) and a reference device that is not irradiated. The outputs of the two devices are compared. The errors are counted and recorded. Static input signals have been applied and only the 7 MSB have been tested.

The device tested did not exhibit SEL up to a LET of 11.4 MeVcm^2/mg, then it is sensitive to SEL at the LET of 20 MeVcm^2/mg. The SEL cross section at the maximum tested LET is about $1x10^{-4}$ cm^2/device. The SEL cross section curve is shown in Figure 11.

The SEU sensitivity of the 4 MSBs is very low. The LET threshold is about 11.2 MeVcm^2/mg and only a few SEU have been observed. The LET threshold of the 3 medium bits (bits 5,6,7) is about 1.8 MeVcm^2/mg and the SEU sensitivity of the three medium bits (bits 5,6,7) dominate the SEU response of the 7 tested bits. We could expect a higher sensitivity of the 5 LSBs that have not been tested. The SEU cross section curve is shown in Figure 11. [T080101_ADC.pdf]

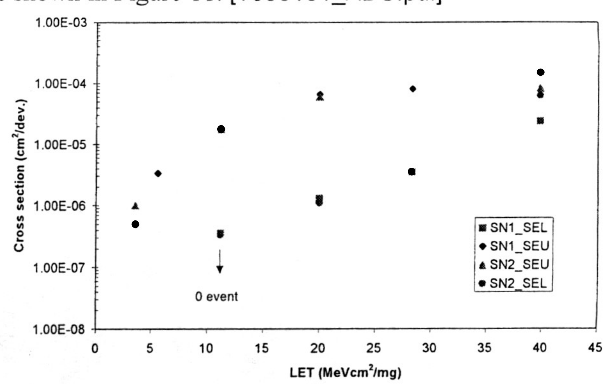

Fig. 11: AD9223 SEU and SEL cross section curve.

4) LTC1272

The 12 bits ADC LTC1272 from Linear Technology was tested for SEU and SEL at TAMU using ions covering a LET range from 1.8 MeVcm^2/mg (Ne at 0 degree) to 20 MeVcm^2/mg (Kr at 0 degree). The test method used is the golden chip. The same input signal is sent to the Device Under Test (DUT) and a reference device that is not irradiated. The outputs of the two devices are compared. The errors are counted and recorded. Static input signals have been applied and only the 7 MSB have been tested.

The device tested is very sensitive to SEL, the SEL LET threshold is lower than 5.6 MeVcm^2/mg and the cross section at the maximum tested LET is 1x10^{-4} cm^2/device. The SEL cross section curve is shown in Figure 12.

The SEU sensitivity of the 3 medium bits tested dominates the SEU response of the 7 tested bits. The LET threshold of the 4 MSBs is about 4 MeVcm^2/mg and the number of errors is low. The LET threshold of the 3 medium bits (bits 5,6,7) is less than 1.8 MeVcm^2/mg and the number of errors is very high. We could expect a higher sensitivity of the 5 LSBs that have not been tested. The SEU cross section curve is shown in Figure 13. [T080101_ADC.pdf]

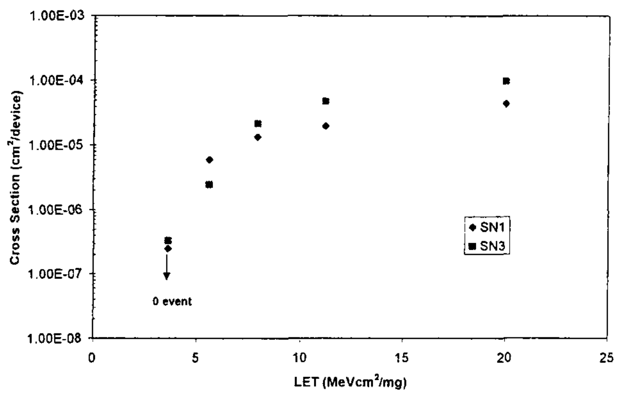

Fig. 12: LTC1272 SEL cross section curve.

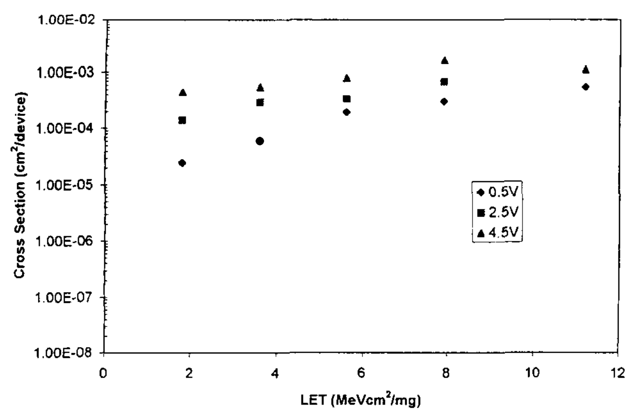

Fig. 13: LTC1272 SEU cross section curve.

5) LTC1657

The 16 bit Digital to Analog Converter LTC1657 from Linear Technology was tested for SEU and SEL at BNL using ions covering a LET range from 3.4 MeVcm^2/mg (Fluorine at 0 degree) to 37 MeVcm^2/mg (Bromine at 0 degree). The set-up allowed the distinction between the transient errors (glitch at the device output) and the permanent errors (Single Event Upset in the device registers). A static digital input has been applied during the irradiation (about mid scale, DUT ouptut=2V). With this set-up we have been able to test the 11 most significant bits out of the 16 bits device resolution.

The device is not sensitive to SEL up to a LET of about 14 MeVcm^2/mg. The SEL cross section is about 6.3E-05 cm^2/device at the LET of 37 MeVcm^2/mg. The SEL cross section curve is shown in Figure 14. During a SEL the part is not functional, but after a power cycle the device recovers its functionality. The latchup current is about 54 mA.

Figure 14 shows the cross section curves of the SEU sensitivity and the total device error sensitivity. Most of the errors are SEU that occur in the device registers, but at high LET a significant number of transient errors are observed. The SEU LET threshold is about 4 MeVcm^2/mg and the cross section is 3.8E-4 cm^2/device at the LET of 37 MeVcm^2/mg. The cross section of the total number of errors is 1.2E-3 cm2/device at the LET of 37 MeVcm^2/mg. [B030302_LTC1657.pdf]

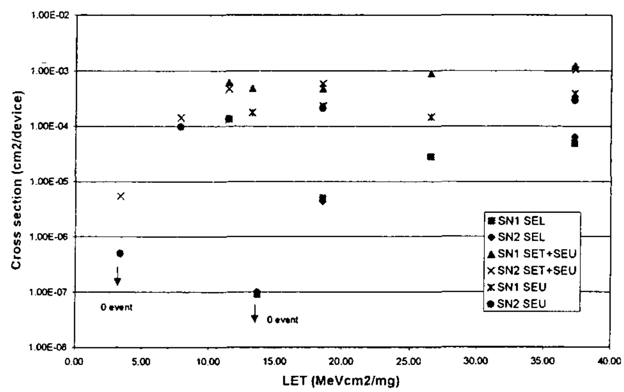

Fig. 14: LTC1657 SEU and SEL cross section curve.

6) ADC1175

The 8 bit Analog to Digital Converter ADC1175 from National Semiconductor was tested for SEU and SEL at BNL and TAMU using ions covering a LET range from 3 MeVcm^2/mg (Ne at 0 degree) to 59 MeVcm^2/mg (Iodine at 0 degree).

The National semiconductor ADC1175 evaluation board has been used for the SEE testing. This board operates the AD1175 from a single +5V supply at a 20 MHz clock. Before each irradiation, the device digital output is stored in a 8 bit register. Then, during the irradiation, the DUT output is compared to the register content. In case of difference, an error is counted. Input voltage during the experiment is 4.5V.

The device is not sensitive to SEL up to a LET of about 23 MeVcm^2/mg. The SEL cross section is about 4.6E-04 cm^2/device at the LET of 118 MeVcm^2/mg. The SEL cross section curve is shown in Figure 15. The latchup current is 86 mA.

The device has a significant SEU/SET sensitivity with a LET threshold lower than 2 MeVcm^2/mg and a device SEU/SET cross section of 4.5E-4 cm^2/device at a LET of 49 MeVcm^2/mg. The SEU/SET cross section curve is shown in Figure 15.

No SEFI was observed during all the experiments. [B030302_ADC1175.pdf]

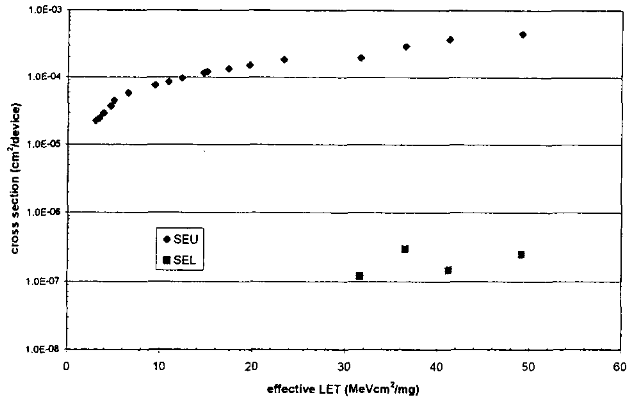

Figure 15: ADC1175, SEU and SEL cross section curve.

E. Communication Devices:

1) 1394 FireWire containing TSB12LV26PZT, and TSB41AB3PFP, from TI and the CS4210VJG, and CS4103VHG from NSC

Radiation tests were performed on IEEE 1394 Open Host Controller Interface (OHCI) Chipsets from two manufacturers, Texas Instruments (TI) and National Semiconductor (NSC), to evaluate Single Event Effects. Four parts were tested in two different modes at three different facilities, Brookhaven National Laboratories (BNL), TRI-University Meson Facility (TRIUMF) and Texas A&M Cyclotron Facility. Many types of SEFI were observed which required intervention to correct from software bus resets to the more severe cable reset and power cycling. Serious mitigation concerns must be addressed in order to use these parts. See [NSREC02_PI-3] and [T101401_1394.pdf]

2) Myrinet

Myrinet crossbar switches and a network interface card (NIC) were exposed to the 63 MeV proton beam at the Crocker Nuclear Lab at the University at California at Davis to perform a proton SEE evaluation. Proton-induced Single Event Upsets (SEUs) and Single Event Functional Interrupts (SEFIs) were observed at the system level for both the crossbar switches and for five devices exposed on the NIC. SEU cross section for the crossbar switch was approximately 5 x 10^{-13} cm^2, on average and ranged from 5 x10^{-12} to 8 x 10^{-11} cm^2 for the NIC, depending on which device was exposed. The SEFI cross section for the crossbar switch was approximately 5 x 10^{-13} cm^2 and ranged from 3 x 10^{-12} to 4 x 10^{-10} cm^2 depending on which device was exposed. The complete details on the testing and results can be found in this year's Data Workshop paper entitled "Proton Single Event Effects (SEE) Testing of the Myrinet Crossbar Switch and Network Interface Card", by J.W. Howard Jr., *et al.* [NSREC02_W-8] and [D112601_Myrinet.pdf]

3) AD8151

SEE testing was carried out at the Texas A&M University Cyclotron Facility. Table 12 shows the heavy ions used for testing.

TABLE 12: IONS USED FOR TESTING THE AD8151 TOGETHER WITH THEIR LETS AND ANGLES OF INCIDENCE.

Ion	LET (MeV.cm^2/mg)	Angles (Degrees)
Ne	2.86	0,45,60
Ar	8.96	0,45,60
Kr	30	0,60

The part was mounted in air on a stage that made it possible to change the angle of incidence, thereby increasing the effective ion LET. A Bit Error-Rate Tester (BERT) was used to provide a serial stream of data ("1s" and "0s") to the input of the AD8151. The signals supplied by the BERT were a standard, pseudo-random 127-bit repeating sequence pattern having a value of – 0.75 V_{dc} with 1.5 V peak-to-peak differential. After passing through the switch, the signals were fed back into the BERT for comparison with the expected signal. High performance cables (18 GHz) were used for all RF signals. Two configurations were tested to evaluate how the BER depended on the number of switches through which the signal passed. In the first configuration a single input was connected through the switch matrix to a single output, i.e., BERT(out) →In(10)→Out(0)→BERT(in). In the second configuration the signal from the BERT passed through the switch five times, i.e., BERT(out)→In(10)→Out(0)→In(13)→Out(2)→In(8)→Out(6)→In(28)→Out(16)→In(18)→Out(10)→BERT(in). The BERT compared the actual output with the expected output to check for any changes in data. That information was stored for later analysis. During the actual runs, the part was started before the beam was switched on. The beam was switched off either after a fixed fluence or immediately following a cessation of transmission, which was heralded by the BERT as a loss of synchronization (LOS). To calculate the bit error rate (BER) the total number of bits transmitted during the exposure time must be known as well as the total number of errors. The total number of transmitted bits was obtained from the product of the data rate and the time the beam was on.

The set of errors obtained from each run was analyzed according to whether they were "non-burst" (single-bit errors) or "burst" errors (a stream of errors). A single burst consists of more than one sequential error and is termed a "burst event." An "non-burst" event contains a single error. The total number of events is the sum of the burst events and the non-burst events.

Generally, the higher the data rate, the lower is the BER. There appears to be a peak in the BER at a LET of 7

MeV.cm^2/mg and then a stead increase with LET at higher LETs. The generally higher bit error rate at the lower LETs is most likely due to the fact that at low LETs most of the errors are non-burst errors, consisting of single bit upsets. At higher LETs most of the events consist of long bursts of errors. Many more non-burst errors (that dominate at low LETs) can be recorded during a fixed time interval than burst errors (that dominate at high LETs).

The AD8151 Cross Point Switch exhibits two types of single-event effects. The first consists of a temporary loss of transmission caused by heavy ion strikes to the switches themselves and resulting in bursts of errors whose length depends on ion LET. The second consists of a complete cessation of transmission caused by heavy ion strikes to the registers containing the data specifying the switch configuration. Only by rewriting the data to the registers can data transmission be restarted. The part is latchup-free to a LET of 60 MeV.cm^2/mg and shows no changes in supply current up to a TID of 14 krad(Si). [T031502_AD8151_paper.pdf] [D013102_AD8151.pdf]

4) LSP2916

The Agere Systems LSP2916 16-channel, high voltage driver for microelectromechanical systems (MEMS) was tested for SEE. Two device types were tested, the "A" version with –33V/V gain and the "B" version with –66V/V gain. The devices were tested at Brookhaven National Laboratory's Single Event Upset Test Facility. The devices showed no evidence of SETs on the output during testing.

The device exhibited a destructive SEE at an LET of 26.6 MeV•cm^2/mg (Ni-58 at normal incidence). No event was observed at an LET of 11.4 MeV•cm^2/mg. Thus, the SEL LET_{th} is between 26.6 MeV•cm^2/mg and 11.4 MeV•cm^2/mg. The SEE rendered the entire device non-functional due to the partial vaporization of the V_{LP} (5V power supply) bond wire (A type, –33V/V gain devices) or the complete vaporization of the V_{LP}, V_{HN} (high voltage negative supply) and Ground bond wires. See Figures 16 and 17 for views of DUT 2 (B type, -66V/V gain devices). When the SEE occurred, in all cases, a spark was visible on the test vacuum chamber closed circuit TV monitor. In the case of one device, the first run with Ni probably caused a momentary melt that self-healed. The subsequent run caused a permanent failure. The analysis of the exact nature of the SEE is under investigation and will be completed shortly. [B122001_LSP2916.pdf]

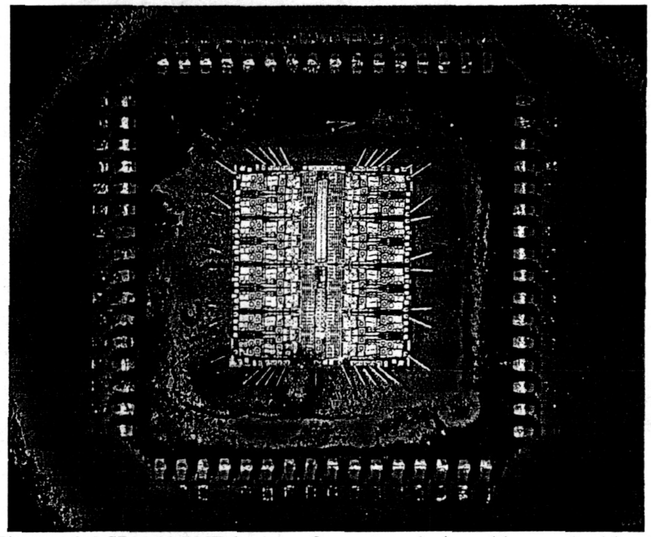

Figure 16. LSP2916 DUT 2 view of complete device with vaporized bond wires.

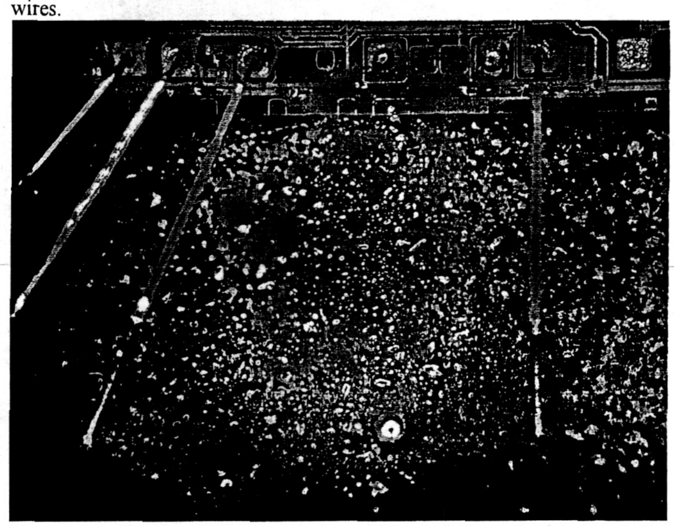

Figure 17. LSP2916 DUT 2 detail view of V_{LP} and Ground wires. Note the spallation of the trace as well.

5) APS Photobit

The Photobit active pixel sensor (APS) was tested for SET at Texas A&M University cyclotron facility. Measurements were made using Ar-40 at 15.0 MeV/amu, Kr-84 at 15.3 MeV/amu, and Xe-131 at 15.2 MeV/amu. The heavy ion single event transient response of Photobit APS subarrays is very dependent on the specific pixel design. No latch-up is observed up to an LET of 106 MeV/mg/cm2 (Xe at 60o) for a fluence >2x107cm2 [NSREC02_LateNews_Marshall_Photobit].

6) Test Sample 5HP SiGe Prescaler

This IBM SiGe Heterojunction Bipolar Transistor (HBT) BiCMOS technologies, 5HP series was tested at CNL (Protons) and TAMU (Heavy Ions). Bit upsets were see at 63MeV protons. For more information see "Single Event Upset Test Results on an IBM Prescaler Fabricated in IBM's 5HP Germanium Doped Silicon Process," [nsrec01_5HP].

7) PE9301

The Peregrine divide-by-2 prescaler fabricated in Ultra Thin Silicon (UTSi) 0.5um Silicon0On0Sapphire (SOS) process was tested at CNL (Protons) and TAMU (Heavy Ions). Bit upsets were see at 63MeV protons. For more information see "Effects of Proton Beam Angle-of-Incidence on Single-Event Upset Cross-Section Measurements," [nsrec02_H-4].

8) MTX8501 and MRX8501

The Emcore MTX8501 Transmitter and MRX8501 Receiver were proton testing at Crocker Nuclear Laboratory using 63 MeV protons.

Both the transmitter and receiver were mounted on individual evaluation boards that minimize stray capacitances and allow for maximum frequency operation. The boards are identified in table 13.

TABLE 13: IDENTIFICATION NUMBERS FOR EVALUATION BOARDS, TRANSMITTER AND RECEIVER

Function	Evaluation Board	Device Serial Number
Transmitter	TX, 1.25GB/S 600864 Rev 4	A1 312-12
Receiver	RX, 1.25GB/S 600863 Rev 4	A1 233-01

Two SMA connectors are required for each channel because the electrical input signals are in the form of differential voltages. The power supply to the board was 5 V, but 3.3 V was derived on the board for powering the parts. The electrical input signal was supplied by the Bit Error Rate Tester (BERT). 62/125 MM FO cables were connected to the output of the transmitter and the input of the detector via MO connectors. An attenuator was inserted in the optical path to reduce the light intensity in order to measure the optical power budget, i.e., how much spare light intensity was available above the point at which there would be a significant increase in the bit error rate caused by noise in the system.

For proton testing, only one channel was used. The electrical signal consisted of a bit stream of logical "1s" and "0s" obtained from a pseudo-random number generator. The transmitter converted the electrical signal into an optical signal, which was transmitted through the optical fiber to a receiver, where it was converted back into an electrical signal. The signal from the detector was compared with that originally supplied to the emitter. Differences were flagged and noted as errors. Before exposing the device-under-test (DUT) to the proton beam, the light intensity arriving at the receiver was adjusted using the attenuator to determine the optical power budget.

In the actual setup, the transmitter and receiver were both located in the target room. The receiver was placed in front of the proton beam because previous experience suggests that the photo-detector, not the VCSEL, is the source of most SEEs. The optical cable from the transmitter in the target room was routed through a conduit in the concrete walls of the target chamber and connected to the attenuator located in the vicinity of the experimenters. The light intensity was measured using a light wave multimeter 8163A from Agilent. The output of the attenuator was routed back through the conduit to the receiver positioned in front of the beam. In this way it was possible to modify the attenuation without having to enter the target chamber.

Each test run involved a different set of experimental parameters, including angle, attenuation and transmission rate. The following are the reasons for varying this set of parameters: i) Detectors with large lateral dimensions are known to exhibit a marked increase in the bit error rate for protons near grazing incidence, i.e., near 90°, due to single-event transients (SETs) caused by direct ionization, ii) the error rate increases with decreasing light intensity, and iii) the error rate increases with increasing data transmission rate.

To facilitate angular measurements, the board with the device-under-test was mounted on a stage with both translational and rotational degrees of freedom. The stage was used both to align the part and to change the angle of incidence.

The proton beam current was selected to be 5000 pA so that there would be sufficient SETs for good statistics and for doing the test in a cost-effective manner. At the same time, there would not be too many either to overwhelm the system or run the danger of multiple hits during the transmission of one bit of data.

Two different receivers (photodiodes) and one transmitter were tested. For testing of the transmitter, the receiver was removed from in front of the accelerator exit port and replaced by the transmitter. The data for the transmitter (Run #67) show that, as expected, SETs are not generated when the transmitter is irradiated with protons.

The BER showed a significant increase when the proton beam was close to grazing incidence. In fact, at an angle of 90 degrees, the increase was greater by more than an order of magnitude over the bit error rate at 20 degrees. The actual BER was found to depend on both the attenuation setting and the data transmission rates. This suggests that SETs in the detectors can be produced via direct ionization by protons traveling over the long paths lengths in the lateral direction of PIN diodes. Ionization from secondary particles produced through collisions between protons and atomic nuclei would not exhibit the enhancement at large angles of incidence.

F. Processor Boards:

1) Pentium PIII 1000, 933, 850, and 800 MHz

During this year, Pentium III (P3) devices ranging in speed from 550 MHz to 1.2 GHz were tested for Single Event Effects (SEE) at four different times at two facilities: Texas

A&M Cyclotron (TAMU) with heavy ions, Indiana University Cyclotron (IU) with protons. Each test added newer generation technology devices and improved software to examine the effects in more detail or to examine unanticipated observed effects.

The final testing done at IU involved the testing of three technology generations (0.25, 0.18, and 0.13 micron) and was done across the entire speed range of 466 MHz to 1.2 GHz (the 466 MHz was achieved by lowering the clock speed on a 700 MHz device). An interesting piece of data observed in this testing involved the L2 cache (see Figure 18). This data points out a major testing issue that arose during both heavy ion and proton testing. The issue was that when the cache was loaded sequentially (Test C) and was run for the 50 and 25 percent cases, a different per-bit cross section was seen. However, when the cache is loaded non-sequentially (Test I), the three percentage cases do not show the same variation. There is nothing in any Intel documentation that indicates any special data fetching, storages, etc., whenever data is continually fetched sequentially. Even is there was, that would not explain why the 100% case Test C is unaffected by whatever mechanism is in place. This data does indicate the importance of thoroughly understanding how data is taken on complex devices, such as the Pentium III to completely understand the test results.

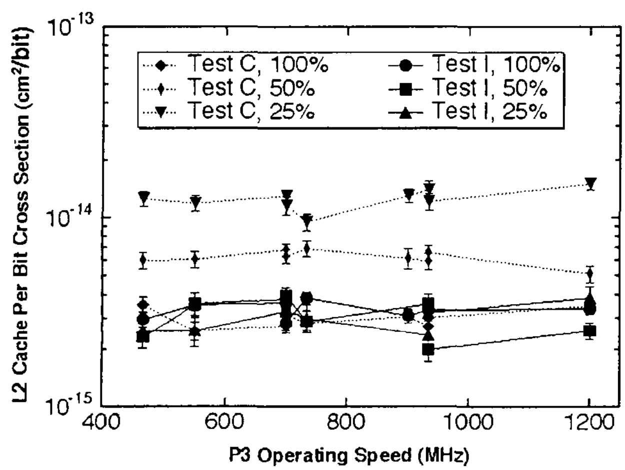

Fig 18: Per Bit L2 Data Cache cross section as a function of P3 operating speed.

Complete test reports are available at the Goddard Radiation Effects & Analysis Group Web site [IU0501.pdf] [TAMU0301.pdf] [T101201_P3.pdf] [IU0600.pdf] [IU1200.pdf]. A summary paper was presented of the earliest work at the 2001 NSREC Data Work Shop and can be found in that Workshop Record [NSREC01_W7.pdf]. Additionally, updated presentations and papers (in the respective proceedings) were made at the 2001 MAPLD and 2002 SEE Symposia [MAPLD01_P3.pdf] [Seesym02_P3.pdf].

V. Single Event Latchup

A. ADCs:

1) LTC1604, LTC1605, LTC1608

These 16 bits Analog to Digital Converters have been tested for SEL. The objective of these tests was to perform a preliminary screening.

- LTC1604 has been tested with a 25 MeV/u Xe beam at TAMU covering a LET range from 40MeVcm^2/mg (0 degree) to 65 MeVcm2/mg (52 degrees). No SEL events were observed for all angles of incidence up to a fluence of 2E6 ions/cm^2.
- LTC1605 has been tested with a 15 MeV/u Xe beam at TAMU covering a LET range from 54 MeVcm^2/mg (0 degree incidence) to 60 MeVcm^2/mg (0 degree incidence,degraded beam). This part showed a very high SEL sensitivity at all LET values. As soon as the beam is turned on the part latches. While the device is latched the part is not functional. The device always recovered its functionality and a normal power supply current after a power cycle.
- LTC1608 has been teted at BNL using ions with effective LET ranging from 60 MeVcm^2/mg (Iodine) to 95 MeVcm^2/mg (Gold at 30 degrees). No SEL event was observed up to a LET of 82 MeVcm^2/mg (Gold at 0 degree) up to a fluence of 1E7 ions/cm^2. 1 SEL has been observed at a LET of 87 MeVcm2/mg (Gold at 20 degrees) for a fluence of 7E6 ions/cm^2. 2 SEL have been observed at a LET of 95 MeVcm^2/mg for a fluence of 8.5E6 ions/cm^2. [T080101_LTC1604.pdf] [T100101_LTC1605.pdf] [B030302_LTC1608.pdf]

B. Misc:

1) ADG452

The analog switch ADG452 from Analog Devices was tested for SEL at BNL using ions covering a LET range from 60 MeVcm^2/mg (Iodine at 0 degree) to 82 MeVcm^2/mg (Gold at 0 degree). No SEL events were observed for all LET values up to a fluence of 1E7 ions/cm^2.

2) ICL7662

The voltage converter ICL7662 from Intersil was tested for SEL at BNL at a LET of 82 MeVcm^2/mg (Gold at 0 degree). No SEL events were observed up to a fluence of 1E7 ions/cm^2.

3) XA1

The XA1 is an Application Specific Integrated Circuit (ASIC) intended to process data from 128 detector elements. The ASIC is designed by IDE As. of Norway and fabricated in 1.2 micron feature size bulk CMOS and two different 0.8 micron CMOS on epitaxial processes by Austria Mikro Systeme International. These devices were tested with a user-provided set up (to ensure fidelity to the application) for susceptibility to heavy-ion and proton induced single-event latchup (SEL). The experimental setup included four separate power supplies that supplied positive and negative biases to the analog and digital portions of the ASIC. For the purposes of this test, a SEL was said to have occurred if any of the power supplies experienced a current spike and the normal functionality of the part was disrupted. The power supplies were configured so that they could operate either with or without current limiting and power cycling in the event of an SEL.

The Bulk ASICs were tested at Brookhaven National Laboratory, and the ASICs implemented on epi processes were tested at the Texas A&M University Cyclotron Institute. The Bulk ASICs were found to be susceptible to SEL with an onset LET of about 5 MeVcm2/mg and a limiting cross section of about 1E-2 cm2. The ASICs on epi processes were found to have an onset LET for SEL of 8 MeVcm2/mg, with a limiting cross section about a factor of 10 smaller than the bulk process.

To determine whether the SEL mode(s) were destructive, several ASICs were tested without current limiting. No ASICs exhibited any destructive SEL modes up to an LET of 37 MeVcm2/mg and a fluence of 1E7 particles/cm2. For LETs above 37, about 3% of the SELs in the bulk ASICs were destructive, perhaps indicating the existence of multiple SEL modes. The ASICs on epi did not exhibit destructive SEL, but due to problems at the cyclotron could only be tested to an LET of 41 MeVcm2/mg.

The low onset LETs of the nondestructive SEL modes suggest that these parts could be susceptible to proton-induced SEL. However, no SELs were observed during tests with 63 MeV protons at the UC Davis proton cyclotron up to the point where the XA1s failed due to TID (1.2-1.8 E11 protons/cm2). Note: The TID degradation did anneal, and the parts were operational by the time they were returned to Goddard Space Flight Center.

4) PCA80C522

The Phillips Processor device PCA80C522 was tested for SEE at BNL. Sample size was one part. For each of the test runs, the device was biased with 5 volts and run at 16 MHz in the idle mode. For all ions used, single event latchup was observed. Latchup currents measured varied from approximately 13 to 90 mA, where current was approximately 300 uA in the idle mode.

The LETth for latchup is approximately 3-5 MeV-cm2/mg and the saturation cross section is approximately 3x10-3 cm-2 or higher. The "or higher" comment comes from the fact that the data taken at the three highest LET points was limited due to the particle flux rates achievable

The second part of the testing was the dwell test. This data is summarized in Table 14. Dwell times of 5, 10, 15, 30 and 60 seconds were used for this testing. For each of these cases, the latchup current was at whatever level occurred (no effort was made to chose the current level for the dwell testing). For the first four time intervals, the processor after having its power cycled resumed normal operation. However, after latching and being allowed to stay in the latched state for 60 seconds, a power cycle would not recover the normal operation (current draw stayed in excess of 15 mA). No number of power cycles or power off times were able to recover the DUT to nominal operation. Therefore, the latchup that occurs in these devices does become destructive if allowed to stay latched for a time in excess of 30 seconds.

It should also be noted that numerous events were observed that required a reset to the PCA80C552 rather than a power cycle. These single event functional interrupts (SEFIs) were not gathered except to note that they occurred. The device was approximately 5-10 times more sensitive to SEFIs than to latchup. [B082301_PCA80C552.pdf]

TABLE 14: SUMMARY OF DWELL TESTING FOR THE PCA80C522

SEL current in mA	Time in seconds of dwell	Recovery?
90	5	yes
58	10	yes
60	15	yes
84	30	yes
26	60	No, hard failure of device

VI. DISPLACEMENT DAMAGE

A. Misc:

1) BAE CCD486

A BAE Systems/Fairchild CCD846 charge-coupled device (CCD) imager was subjected to proton testing for the Hubble Space Telescope Advanced Camera for Surveys (ACS) program. The CCD486 is a 4k x 4k, full frame, n-channel, 15μ pixel pitch imager with a 3μ supplemental implant (mini-channel) in both the vertical and horizontal registers. The imager was irradiated with 63 MeV protons at the University of California at Davis Crocker Nuclear Laboratory. Two different regions of the CCD were exposed to fluences of 2.5e9 p/cm^2 and 5e9 p/cm^2 using a moveable metal mask. The irradiations were carried out at room temperature with the imager unbiased. Pre- and post-rad characterization was performed in the Ball Aerospace and Technologies Corporation ACS CCD characterization facility. Parallel First Pixel Response (FPR) CTE measurements taken at –81 °C exhibit simple power law behavior as a function of signal level except for a slight change in the slope of the 5e9 p/cm2 curve at low signal levels. As in previous studies, FPR is found to be in good agreement with ^{55}Fe at a signal level of 1620 electrons. Serial FPR measurements for the 2.5e9 p/cm^2 half of the imager show a bump in the CTE curve at high signal levels that results in a decrease in CTE (or an increase in CTI). The parallel and serial measurements are compared in Figure 19.

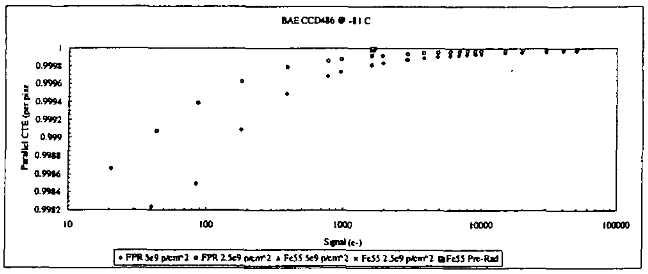

(a)

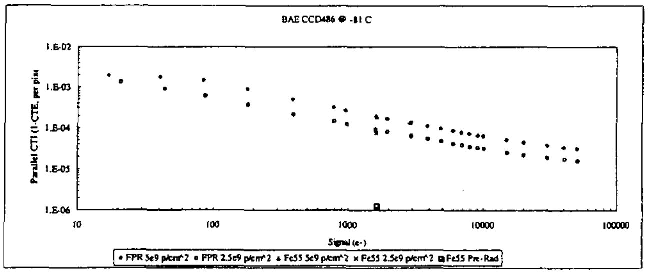

(b)

Figure19: BAE CCD486 radiation test results: (a) parallel CTE, (b) Parallel CTI.

We interpret the bump as an indication that the signal packet, confined in the horizontal register mini-channel at low signal levels, has reached the overflow capacity of the mini-channel. The decrease in CTE is caused by the increase in the signal packet volume as the charge expands beyond the edge of the mini-channel. We speculate that a similar CTE characteristic does not occur in the vertical register because the vertical shift rate is much slower than the horizontal shift rate. For this test, the serial shift rate was 22 μsec/pixel and the vertical shift rate was 91 msec/row. The much slower vertical shift rate may allow carriers confined in the mini-channel time to escape into the main channel before the charge packet is transferred into the next pixel. [D030701_CCD486.pdf]

2) TIL25

Figure 20 shows the degradation (P/P_o) of both LEDs at each exposure level (fluence) when V_{IN}=3.3V and I_F=35mA. The measured output power (P) for each LED at each fluence level is normalized to the pre-irradiation output power (P_o). There is a significant amount of degradation seen in both of devices after receiving a total fluence of $2.56x10^{10}$p/cm^2. Following the final step (total fluence is $1.53x10^{11}$p/cm^2), the device performance has degraded significantly, to less than 15% of its initial value. This degradation curve is characteristic of a single heterojunction LED. [D040101_TIL25.pdf]

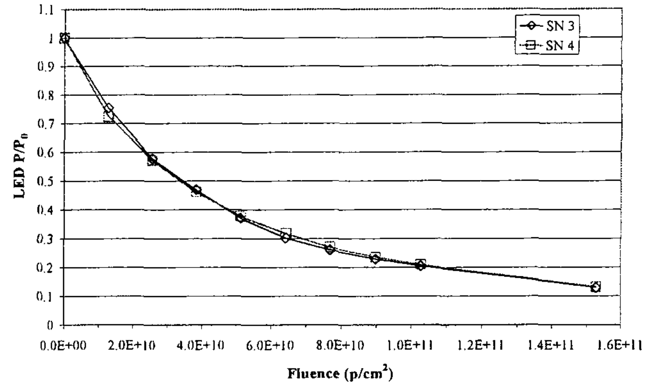

Figure 20. Proton induced degradation of LED power output for both TIL25 devices. The LED output power was normalized to the pre-radiation values.

3) TIL601

The Texas Instruments TIL601 is an N-P-N planar silicon phototransistor. Two samples were tested (SN3 and SN4). These devices are discreet components therefore no delidding was needed prior to exposure. The devices were exposed to protons at the University of California at Davis Crocker Nuclear Laboratory. The phototransistor output was monitored for radiation-induced degradation at various fluence levels. Figure 21 shows the degradation (I/I_o) of both phototransistors at each exposure level (fluence) when V_{CC}=5.0V. The current (I) is measured across the load R2 following the phototransistor at each fluence level and is normalized to the pre-irradiation current (I_o). There is a significant amount of degradation seen in both devices after $6.4x10^{10}$p/cm^2. Following the final step (total fluence is $1.53x10^{11}$p/cm^2), the device performance has degraded significantly, to less than 30% of its initial value. [D040101_TIL601.pdf]

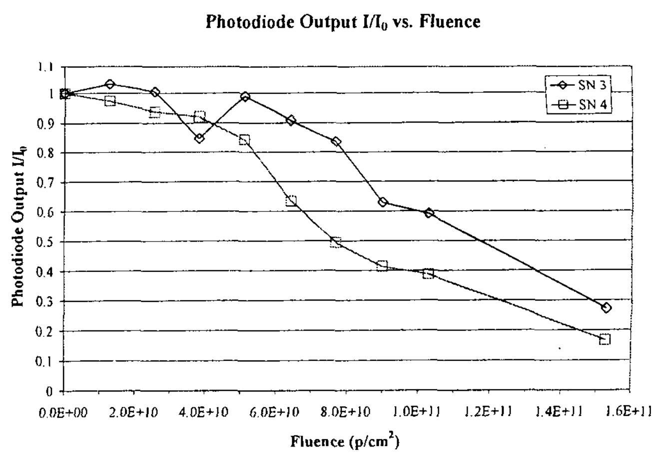

Figure 21. Proton induced degradation of the current for both TIL601 phototransistors. The photodiode current was normalized to the pre-radiation values.

4) 4N49

Three samples of Mii 4N49 optocouplers were tested at the University of California at Davis, Crocker Nuclear Laboratory (CNL) on 01-02 May 2001. The devices were exposed to protons in the CNL cyclotron facility. The purpose of this test was to provide upper and lower bounds for the degradation of the parameter V_{CE} in the Micropac 4N49 optocoupler devices (LDCs 9803 and 9818).

The DUTs were irradiated unbiased with 63MeV protons and then tested after each step by sweeping through various V_{IN} and V_{CC} to determine the change in V_{CE} for those conditions. The devices were operated with a custom setup through a GPIB controller and a laptop. V_{CC} was swept from 22V to 34V in 1V steps with V_{IN} held constant for each V_{IN} value. V_{IN} values ranged from 3.6V to 5.1V in 0.1V increments. The total number of measurements per DUT per run was 208. In all, six step irradiations were performed on the samples.

The project gave the following conditions as input test parameter bounds: $V_{CC\ MIN}$ = 24V, $V_{CC\ Nom}$ = 28V, $V_{CC\ MAX}$ = 34V, and $V_{IN\ MIN}$ = 3.6V, $V_{IN\ Nom}$ = 4.5V, $V_{IN\ MAX}$ = 5.1V. The resulting V_{CE} is the test result of interest for the project. For the purposes of presenting results in an interpretable manner, V_{CE} is presented at the maximum, nominal and minimum values for V_{CC} and V_{IN} (in all 9 combinations) in order to bound the range of V_{CE}. Assuming a maximum acceptable value for V_{CE} of 2.4V, there are no issues as the IRAC 90% confidence level requirement is $3x10^{10}p/cm^2$. At $1x10^{11}p/cm^2$, V_{IN} is the driving factor in greater than acceptable V_{CE} values. In order for the device to remain within specifications, higher V_{IN} values would be preferred. Table 15 gives the average V_{CE} for all thee devices' worst, nominal and best cases. [D050101_4N49.pdf]

TABLE 15: IRAC SUMMARY TABLE:

	V_{CC}	V_{IN}	Initial V_{CE}	Avg. V_{CE} at $1x10^{10}$	Avg. V_{CE} at $3x10^{10}$	Avg. V_{CE} at $5x10^{10}$
Worst Case	34V	3.6V	0.136 ±0.006V	0.158 ±0.004V	0.199 ±0.005V	0.273 ±0.002V
Nominal	28V	4.5V	0.116 ±0.005V	0.134 ±0.003V	0.166 ±0.003V	0.204 ±0.003V
Best Case	24V	5.1V	0.104 ±0.004V	0.121 ±0.003V	0.149 ±0.002V	0.182 ±0.002V

VII. TOTAL IONIZING DOSE (TID)

A. ADCs:

1) AD7714

The 24 bits ADC AD7714 from Analog Devices was tested to total dose up to a dose of 20 krad at a dose rate of 0.86 rad/s. Tests have been performed at NAVSEA/CRANE laboratories. Two devices were statically biased, three dynamically biased Results of the total dose testing indicate:

- Both devices biased statically and all three devices biased dynamically failed and became non-functional between 10Krad(Si) and 20Krad(Si).
- Both devices biased statically and all three devices biased dynamically began showing degradation between 7.5 Krad(Si) and 20Krad(Si) as evidenced by increasing power supply currents. Figure 22 shows the degradation versus dose of the standby current.
- Both devices biased statically and all three devices biased dynamically performed to specified effective resolution of greater than 17 bits up to 10 Krad(Si).
- Both devices biased statically and all three devices biased dynamically showed no degradation in integral nonlinearity up to 10Krad(Si).
- After the 168 hour biased room temperature anneal, all five devices remained nonfunctional. [N032902_AD7714.pdf]

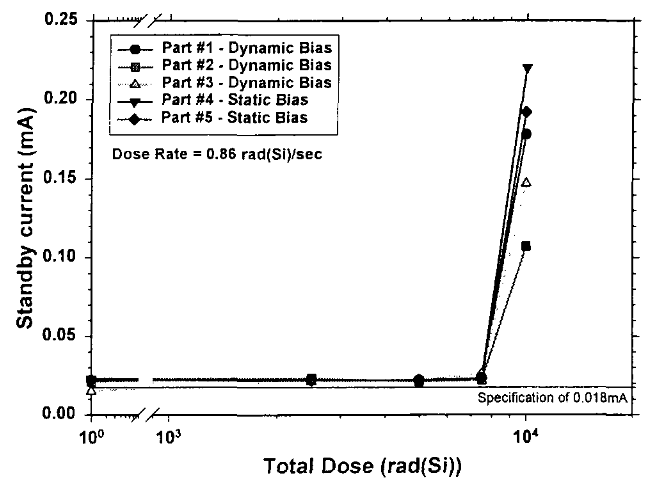

Fig. 22: AD7714 degradation of the standby current verus total dose.

2) LTC1272

The 12 bits ADC LTC1272 from Linear Technology was tested to total dose up to a dose of 30 krad at a dose rate of 0.83 rad/s. Tests have been performed at NAVSEA/CRANE laboratories. Two parts were statically biased, six dynamically biased. Results of the total dose testing indicate:

- Both devices biased statically and one device biased dynamically had missing codes at 7.5krad(Si).
- Both devices biased statically showed degradation in effective number of bits at 7.5krad(Si). Three devices biased dynamically showed degradation in effective number of bits at 7.5krad(Si).
- Both devices biased statically had (maximum) differential non-linearity greater than +1.0 (specification limit) at 5krad(Si). Five devices biased dynamically had (maximum) differential non-linearity greater than 1.0 at 7.5krad(Si). See figure 23.
- Parametric shifts were observed at 5krad(Si).
- All eight devices were still functional, though at a significantly degraded performance level, at 30krad(Si) See figure 24.

After a 168-hour biased room temperature anneal, all eight devices showed a significant improvement in performance, but did not improve to pre rad levels. [N121901_LTC1272.pdf]

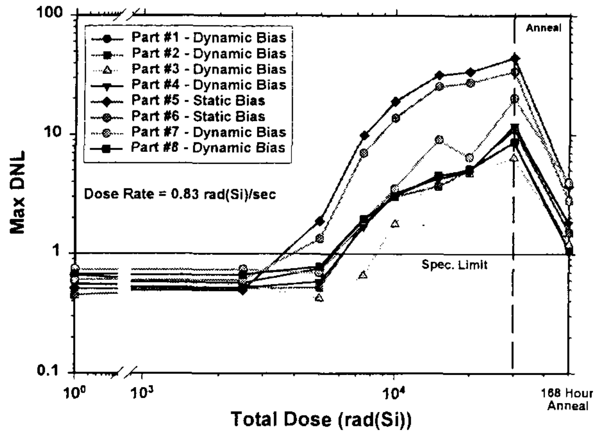

Fig 23: LTC1272 degradation of the differential non linearity versus dose.

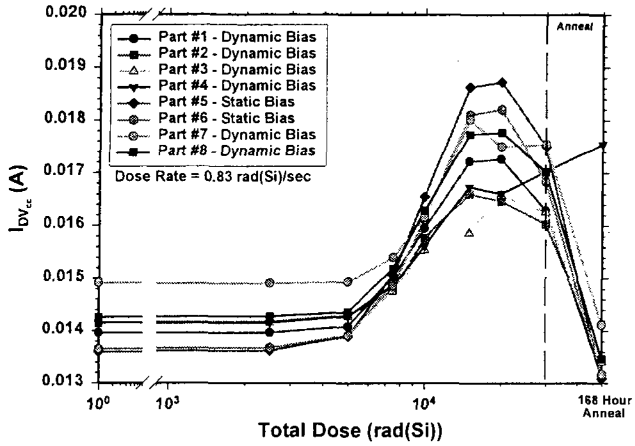

Fig. 24: LTC1272 degradation of the differential supply current versus dose

3) AD6640

NAVSEA Crane Division performed total dose testing on a total of five Analog Devices AD6640, 12 bit ADC's. Three parts were tested with a static bias applied during irradiation and the remaining two parts were tested with a dynamic bias applied. Static bias devices were irradiated with nominal DC power applied and the clock, and all other inputs grounded. Dynamic bias used the same nominal DC power as the static bias condition, a 62.5 MHz Encode clock signal and a 1 MHz, 1.7 volt peak-to-peak amplitude sinusoidal input signal.

The AD6640 experienced no functional or parametric failures up to 30krad(Si). Two AD6640s were tested to 100krad(Si) and no functional or parametric failures were observed. No significant changes in aperture uncertainty jitter were noted up to 30krad(Si), nor for the two devices tested up to 100krad(Si). [N103001_AD6640.pdf]

B. Power MOSFETs:

1) FDN361AN

The 30V 0.15 ohms N channel MOSFET transistor from Fairchild was tested to total dose up to a dose of 50 krad at a dose rate < 1 rad/s. Tests have been performed at NAVSEA/CRANE laboratories. Test results indicate that IDSS increased to a maximum of 32 uA at 50 krds and decreased to 17 uA after anneal; RDSON decreased slightly to a minimum of 0.1 ohms at 50 krds and to 0.098 ohms after anneal; and VGSTH decreased to a minimum of 0.23 V at 50 krds and to 0.28 after anneal. The degradation versus dose of the threshold voltage is shown in Figure 25. [N123101_FDN361AN.pdf]

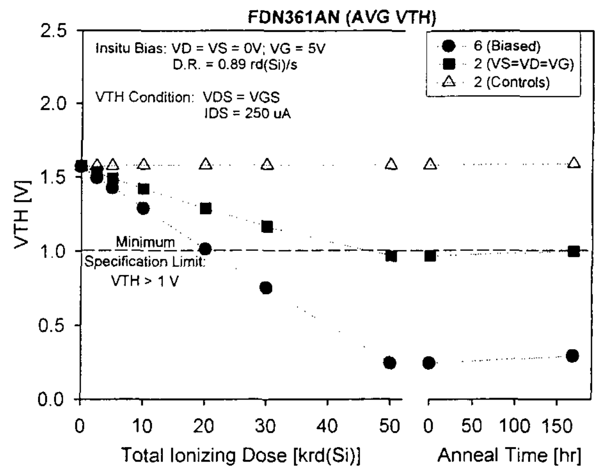

Fig. 25: degradation of threshold voltage versus dose.

2) NDS352A

The 30V 0.5 ohms P channel MOSFET transistor from Fairchild was tested to total dose up to a dose of 50 krad at a dose rate < 1 rad/s. Tests have been performed at NAVSEA/CRANE laboratories. Test results indicate the following that IDSS increased to a maximum of 522 pA at 50 krds and to 575 pA after the anneal; RDSON increased to a maximum of 0.98 ohms at 50 krds and to 0.91 ohms after the anneal; and VGSTH increased to a maximum of -2.63 V at 50 krds and to -2.61 after the anneal. [N123101_NDS352A.pdf]

3) IRLML2803A

The 30V 0.25 ohms N channel MOSFET transistor from International Rectifiers was tested to total dose up to a dose of 50 krad at a dose rate < 1 rad/s. Tests have been performed at NAVSEA/CRANE laboratories. Test results indicate that IDSS increased to a maximum of 442 nA at 50 krds and to 10.8 nA after anneal; RDSON decreased slightly to a minimum of 0.23 ohms at 50 krds but increased slightly to 0.29 ohms after anneal; and VGSTH decreased to a minimum of 0.67 V at 50 krds and to 1.15 V after anneal. The degradation versus dose of the threshold voltage is shown in Figure 26. [N123101_IRLML2803A.pdf]

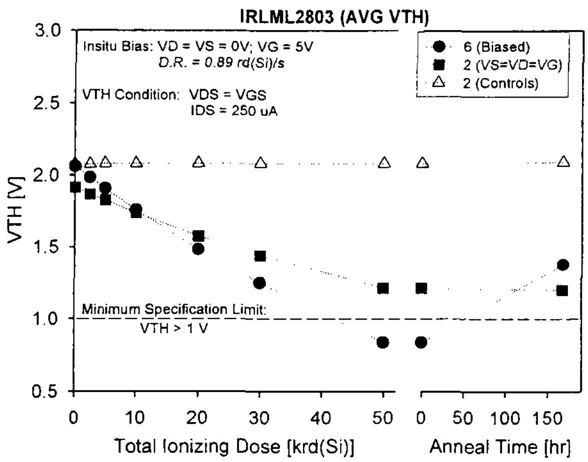

Fig. 26: degradation of threshold voltage versus dose

4) IRLML5103A

The 30V 0.6 ohms P channel MOSFET transistor from International Rectifiers was tested to total dose up to a dose of 50 krad at a dose rate < 1 rad/s. Tests have been performed at NAVSEA/CRANE laboratories. Test results indicate the following that IDSS increased to a maximum of 240 pA at 50 krds and to 555 pA after the anneal; RDSON increased to a maximum of 55 ohms at 50 krds and to 54 ohms after the anneal; and VGSTH increased to a maximum of -3.15 V at 50 krds and to -3.14 after the anneal. [N123101_IRLML5103A.pdf]

C. Processor Boards:

1) Intel Pentium III

Several different speeds (550; 650; 700; 800; 850; 933 MHz and 1 GHz) of the Pentium III Intel processors were tested at the GSFC-REF facility. Biased and operating levels are 500-800 krads(Si). Unbiased failure levels >3 Grads(Si) [G020802_P3_TID.pdf]

D. Miscellaneous Devices:

1) 2N5114

The 40V P channel JFET transistor was tested to total dose up to a dose of 50 krad at a dose rate < 1 rad/s. Tests have been performed at NAVSEA/CRANE laboratories. Test results indicate that only IDSS and IGSS were sensitive to total ionizing dose effects at levels up to 50 krad(Si). Both of these parameters exceeded their specification limit at 50 krad(Si). The bias condition that produced the largest change was VD=VS=VG=0 volts. IDSS increased from 5.2 to 555 pA at 50 krad(Si) and to 584 pA after anneal. IGSS increased from 8.5 to 994 pA at 50 krad(Si) and to 1080 pA after anneal. RDS_ON slightly increased from 60 to 62 ohms at 50 krad(Si) and after anneal. VGS_OFF increased from 7.70 to 7.75 volts at 50 krads(Si) and to 7.85 V after anneal. [N013102_2N5114.pdf]

2) AD8151

The aim of the proton testing was to assess the switch's sensitivity to single-event effects (SEEs) and to total ionizing dose (TID). A single part was tested at Crocker Nuclear Laboratory using 63 MeV protons. SEEs were manifest either by incorrect data appearing at the output of the switch, termed single-event transient (SET), or by a loss of synchronization (LOS), termed a single-event functional interrupt (SEFI). The degree of TID damage was related to changes in the operating current (I_V_{ee}), which was continuously monitored during exposure and by the degradation of signal quality.

A bit error-rate tester (BERT) was used for SEE testing of the switch. The BERT supplied a stream of data to the switch input. The output of the switch was fed back to the BERT and compared with the input. Any differences were flagged as SETs. The signals supplied by BERT were 0.3 V peak-to-peak, NRZ, with an offset of -0.15 V. The data rate could be varied. High performance cables were used for connecting the outputs to the inputs and for connecting the switch to the BERT's.

The switch was programmed using the software supplied by the manufacturer. Two different matrix configurations were used. In the first the data stream passed from an input to an output through a single path defined by a single point connection in the matrix. In the second the data was passed through the switch five times by connecting outputs with inputs and setting five different internal matrix connections. The longer path length meant that there were more possibilities for SETs generated within the switch matrix as well as more sites in the latch that could lead to SEFIs, or loss of synchronization (LOS) as the path continuity is disrupted.

The AD8151 was tested for SEE and TID sensitivity using protons. There were two types of SEEs – data errors that we classified as SETs and losses of synchronization we classified as SEFIs. The error rate depended on data rate but showed very little dependence on the number of paths through the switch. Degradation in the performance of the switch was noticed at about 70 krad(Si) and the operating current increased with dose up to 168 krad(Si). At that level of TID the part still operated, but with reduced performance as evidenced by repeated adjustment of the delay in the window to obtain error-free operation in the absence of radiation. [T031502_AD8151_ paper.pdf] [D013102_AD8151.pdf]

VIII. Summary

We have presented recent data from SEE, and proton-induced damage tests on a variety of mainly commercial devices. It is the authors' recommendation that this data be used with caution. We also highly recommend that lot testing be performed on any suspect or commercial device.

IX. ACKNOWLEDGMENT

The Authors would like to acknowledge the sponsors of this effort: NASA Electronics Radiation Characterization (ERC) Project, a portion of NASA Electronic Parts and Packaging Program (NEPP), NASA Flight Projects, NASA Remote Exploration and Experimentation (REE) Project, and the Defense Threat Reduction Agency (DTRA) under IACRO 01-4050/0001278.

X. REFERENCES

[1] NASA/GSFC Radiation Effects and Analysis home page, http://radhome.gsfc.nasa.gov

[2] [NRL01MAY_LM124.pdf] K. A. LaBel, et al., "Single event transients in LM124 operational amplifier laser test report," http://radhome.gsfc.nasa.gov/radhome/papers/NRL01MAY_LM124.pdf, May 2001.

[3] [nsrec01_ph2] C. Poivey, et al., " Development of a test methodology for single event transients (SET) in lnear devices," IEEE Trans. Nucl. Sci., vol. 48, pp. 2180-2186, December 2001.

[4] [B122101_paper_ lm119.pdf] S. Buchner, et al., "Single-event transient characterization of *LM119* voltage comparator," http://radhome.gsfc.nasa.gov/radhome/papers/B122101_paper_LM119.pdf, December 2001.

[5] [B122101_lm119.pdf] S. Buchner, et al., "Test report: single-event transient characterization of LM119 voltage comparator," http://radhome.gsfc.nasa.gov/radhome/papers/B122101_LM119.pdf, December 2001.

[6] [B030402_22V10.pdf] S. Kniffin et al., 'Heavy ion single event effects test results for three candidate 22V10 reprogrammable logic devices," http://radhome.gsfc.nasa.gov/radhome/papers/B030402_22V10.pdf, March 2002

[7] [B030402_AN10E40.pdf] A. Sanders, et al., "Heavy ion single event effects test results for Anadigm AN10E40 field programmable analog array (FPAA)," http://radhome.gsfc.nasa.gov/radhome/papers/B030402_AN10E40.pdf, March 2002

[8] [T100115_MDI05.pdf] J. Howard, et al., " Single event transient and destructive single event effects re-testing of the MDI3051RES05ZF Modular Devices, Inc. DC/DC converters (with radiation hardened MOSFET)," http://radhome.gsfc.nasa.gov/radhome/papers/T100115_MDI05.pdf, October 2001

[9] [T100115_MDI12.pdf] J. Howard, et al., " Single event transient and destructive single event effects re-testing of the MDI3051RED12ZF Modular Devices, Inc. DC/DC converters (with radiation hardened MOSFET)," http://radhome.gsfc.nasa.gov/radhome/papers/T100115_MDI12.pdf, October 2001

[10] [T100115_MDI15.pdf] J. Howard, et al., "Single event transient and destructive single event effects re-testing of the MDI3051RED15ZF Modular Devices, Inc. DC/DC converters (with radiation hardened MOSFET)," http://radhome.gsfc.nasa.gov/radhome/papers/T100115_MDI15.pdf, October 2001

[11] [B030302_LM2651.pdf] C. Poivey, and Z. Kahric, "Heavy ion single event effects test of switching regulator LM2651 from National Semiconductor," http://radhome.gsfc.nasa.gov/radhome/papers/B030302_LM2651.pdf, March 2002

[12] [B030302_MSK5042.pdf] C. Poivey, et al., "Heavy ion single event effects test of 4A adjustable switching regulator MSK5042 from M. S. Kennedy," http://radhome.gsfc.nasa.gov/radhome/papers/B030302_MSK5042.pdf, March 2002

[13] [B030302_LP3470.pdf] C. Poivey, et al., Heavy ion single event effects test of power on reset LP3470 from National Semiconductors," http://radhome.gsfc.nasa.gov/radhome/papers/B030302_LP3470.pdf, March 2002

[14] [T080101_ADC.pdf] C. Poivey et al., "Heavy ion single event effects test of 8 bits ADC AD7821 from Analog Devices 12 bits ADC AD9223 from Analog Devices 12 bits ADC LTC1272 from Linear Technology," http://radhome.gsfc.nasa.gov/radhome/papers/T080101_ADC.pdf, August 2001

[15] [B030302_LTC1657.pdf] C. Poivey, and J. Forney, "Heavy ion single event effects test of 16 bits DAC LTC1657 from Linear Technology," http://radhome.gsfc.nasa.gov/radhome/papers/B030302_LTC1657.pdf

[16] [B030302_ADC1175.pdf] C. Poivey et al., "Heavy ion single event effects test of 8 bits ADC AD1175 from National Semiconductor," http://radhome.gsfc.nasa.gov/radhome/papers/B030302_ADC1175.pdf, March 2002

[17] [NSREC02_PI-3] C. Seidleck et al., "Test methodology for characterizing the SEE sensitivity of a commercial IEEE 1394 serial bus (FireWire)," NSREC02_PI-3 accepted for publication in IEEE Trans. Nucl. Sci., December 2002.

[18] [T101401_1394.pdf] H. Kim et al., "Single-event effects test report on IEEE 1394," http://radhome.gsfc.nasa.gov/radhome/papers/T101401_1394.pdf, October 2001.

[19] [NSREC02_W-8] J.W. Howard et al., "Proton Single Event Effects (SEE) Testing of the Myrinet Crossbar Switch and Network Interface Card," NSREC02_W-8 accepted for publication in IEEE NSREC 2002 Data Workshop, July, 2002.

[20] [D112601_Myrinet.pdf] J. Howard et al., "Proton Single Event Effects (SEE) Testing of the Myrinet Crossbar Switch and Network Interface Card," http://radhome.gsfc.nasa.gov/radhome/papers/D112601_Myrinet.pdf, November 2001.

[21] [T031502_AD8151.pdf] J. Howard, M. Carts, and S. Buchner, "Heavy-Ion Testing of the AD8151 Cross-Point Switch," http://radhome.gsfc.nasa.gov/radhome/papers/T031502_AD8151.pdf, March 2002.

[22] [T031502_AD8151_paper.pdf] S. Buchner, J. Howard, M. Carts, and K. Label, "Single-Event Testing of the AD8151 Digital Crosspoint Switch," submitted for publication in IEEE Trans. Nucl. Sci., December 2002.

[23] [D013102_AD8151.pdf] P.W. Marshall, M. Carts and S. Buchner, "Proton Testing of the AD8151 Cross-Point Switch," http://radhome.gsfc.nasa.gov/radhome/papers/D013102_AD8151.pdf, January 2002.

[24] [B122001_LSP2916.pdf] Scott Kniffin, Zoran Kahric, and Hak Kim, "Heavy Ion Single Event Effects Test Results for Agere LSP2916 16-Channel, High Voltage Driver (MEMS)," http://radhome.gsfc.nasa.gov/radhome/papers/B122001_LSP2916.pdf, December 2001.

[25] [NSREC02_LateNews_Marshall_Photobit] P.W. Marshall, W.B. Byers, C. Conger, E.S. Eid, G. Gee, M.R. Jones, C.J. Marshall, and R.A. Reed, "Heavy Ion Transient Characterization of a Photobit Hardened-by-Design Active Pixel Sensor Array," accepted for publication in IEEE NSREC 2002 Data Workshop, July, 2002.

[26] [nsrec01_5HP] R. A. Reed, P.W. Marshall, H. Ainspan, C.J. Marshall, and H.S. Kim, "Single event upset test results on a prescalar fabricated in IBM's 5HP silicon germanium heterojuction bipolar transistors BiCMOS technology," IEEE NSREC 2001 Data Workshop, pp. 172-176, July, 2001.

[27] [nsrec02_H-4] R.A. Reed, P.W. Marshall, P.J. McNulty, B. Fodness, H. Kim, R. Reedy, G. Wuo, J. Swonger, and C. Tabbert, "Effects of proton beam angle-of-incidence on singel-event upset cross-section measurements," accepted for publication in IEEE Trans. Nucl. Sci., December 2002.

[28] [IU0501.pdf] J. Howard, K. LaBel, M. Carts, R. Stattel, C. Rogers, and T. Irwin, "Proton single event effects testing of the Intel Pentium III (P3) microprocessors," http://radhome.gsfc.nasa.gov/radhome/papers/IU0501.pdf, May 2001.

[29] [TAMU0301.pdf] J. Howard, K. LaBel, M. Carts, R. Stattel, C. Rogers, and T. Irwin, "Heavy ion single event effects testing of the Intel Pentium III (P3) and AMD K7 microprocessors," http://radhome.gsfc.nasa.gov/radhome/papers/TAMU0301.pdf

[30] [T101201_P3.pdf] J. Howard, K. LaBel, M. Carts, R. Stattel, C. Rogers, and T. Irwin, "Heavy ion single event effects testing of the Intel Pentium III (P3) microprocessor," http://radhome.gsfc.nasa.gov/radhome/papers/T101201_P3.pdf

[31] [IU0600.pdf] J. Howard, E. Webb, K. LaBel, M. Carts, R. Stattel, and C. Rogers, "Proton dose and single event effects testing of the Intel Pentium III (P3) and AMD K7 microprocessors," http://radhome.gsfc.nasa.gov/radhome/papers/IU0600.pdf, June 2000.

[32] [IU1200.pdf] J. Howard, K. LaBel, M. Carts, R. Stattel, and C. Rogers, "Single event effects testing of the Intel Pentium III (P3) and AMD K7 microprocessors," http://radhome.gsfc.nasa.gov/radhome/papers/IU1200.pdf, December 2000.

[33] [NSREC01_W7.pdf] J.W. Howard, M.A. Carts, R.Stattel, C.E. Rogers, T.L. Irwin, C. Dunsmore, J.A. Sciarini, and K.A. LaBel, "Total dose and single event ettects testing of the Intel Pentium III (P3) and AMD K7 microprocessors," NSREC01_W7.pdf, IEEE NSREC 2001 Data Workshop, pp. 38-47, July, 2001.

[34] [MAPLD01_P3.pdf] J.W. Howard, M.A. Carts, K.A. LaBel, T.L. Irwin, J.A. Sciarini, and C. Dunsmore, "Uptate to total dose and single event effects testing of the Intel Pentium III (P3) and AMD K7 microprocessors," MAPLD01_P3.pdf, 2001 MAPLD International Conference Proceedings CD, September 2001.

[35] [Seesym02_P3.pdf] J. Howard, K. LaBel, M. Carts, R. Stattel, C. Rogers, and T.L. Irwin, "Single event effects testing of the Intel Pentium III (P3) microprocessor," Seesym02_P3.pdf, Thirteeneth Biennial Single-Event-Effects (SEE) Symposium Proceedings CD, April 2002.

[36] [T080101_LTC1604.pdf] C. Poivey, and C. Palor, "Preliminary heavy ion single event effects test of ADC 16 bits LTC1604 from Linear Technology," http://radhome.gsfc.nasa.gov/radhome/papers/T080101_LTC1604.pdf, August 2001.

[37] [T100101_LTC1605.pdf] C. Poivey, C. Palor, and J. Howard, "Preliminary heavy ion single event effects test of ADC 16 bits LTC1605 from Linear Technology," http://radhome.gsfc.nasa.gov/radhome/papers/T100101_LTC1605.pdf, October 2001.

[38] [B030302_LTC1608.pdf] C. Poivey, S. Kniffin, and C. Palor, "Preliminary heavy ion single event effects test of ADC 16 bits LTC1608 from Linear Technology," http://radhome.gsfc.nasa.gov/radhome/papers/B030302_LTC1608.pdf, March 2002.

[39] [B082301_PCA80C552.pdf] J. Howard, K. LaBel, J. Forney, and H. Kim, "Single event latchup testing of the PCA80C552 Phillips Processor," http://radhome.gsfc.nasa.gov/radhome/papers/B082301_PCA80C552.pdf, August 2001.

[40] [D030701_CCD486.pdf] M. Jones, R. Schrein, M. Sirianni, and P. Vu, "BAE Systems Charge Coupled Device Radiation Test Results," http://radhome.gsfc.nasa.gov/radhome/papers/D030701_CCD486.pdf

[41] [D040101_TIL25.pdf] J. Howard, R. Reed, S. Kniffin, H. Kim, and P. Marshall, "Proton displacement testing of the TIL 25 LED," http://radhome.gsfc.nasa.gov/radhome/papers/D040101_TIL25.pdf, April 2001.

[42] [D040101_TIL601.pdf] J. Howard, R. Reed, S. Kniffin, H. Kim, and P. Marshall, "Proton displacement testing of the TIL601 phototransistor," http://radhome.gsfc.nasa.gov/radhome/papers/D040101_TIL601.pdf, April 2001.

[43] [D050101_4N49.pdf] S. Kniffin, P. Marshall, and H. Kim, "Report for VCE Degradation in Mii 4N49 Optocouplers for IRAC," http://radhome.gsfc.nasa.gov/radhome/papers/D050101_4N49.pdf, May 2001.

[44] [N032902_AD7714.pdf] J.P. Bings, "NAVSEA AD7714YRU Total Dose Test Report," http://radhome.gsfc.nasa.gov/radhome/papers/N032902_AD7714.pdf, March 2002.

[45] N121901_LTC1272.pdf J.P. Bings, "NAVSEA LTC1272 total dose test report," http://radhome.gsfc.nasa.gov/radhome/papers/N121901_LTC1272.pdf, December 2001.

[46] N103001_AD6640.pdf J.P. Bings, "NAVSEA AD6640 total dose test report," http://radhome.gsfc.nasa.gov/radhome/papers/N103001_AD6640.pdf, October, 2001.

[47] N123101_FDN361AN.pdf J. Titus, "NAVSEA Crane radiation test report no: NSWC C6054-FDN361AN-0001," http://radhome.gsfc.nasa.gov/radhome/papers/N123101_FDN361AN.pdf, December 2001.

[48] N123101_NDS352A.pdf J. Titus, "NAVSEA Crane radiation test report no: NSWC C6054-NDS352AP-0001," http://radhome.gsfc.nasa.gov/radhome/papers/N123101_NDS352A.pdf, December 2001.

[49] N123101_IRLML2803A.pdf J. Titus, "NAVSEA Crane radiation test report no: NSWC C6054-IRLML2803-0001," http://radhome.gsfc.nasa.gov/radhome/papers/N123101_IRLML2803A.pdf, December 2001.

[50] N123101_IRLML5103A.pdf J. Titus, "NAVSEA Crane radiation test report no: NSWC C6054-IRLML5103-0001," http://radhome.gsfc.nasa.gov/radhome/papers/N123101_IRLML5103A.pdf, December 2001.

[51] G020802_P3_TID.pdf J. Howard, K. LaBel, M. Carts, R. Stattel, C. Rogers, T. Irwin and Z. Kahric, "Total Ionizing Dose Testing of the Intel Pentium III (P3) and AMD K7 Microprocessors," http://radhome.gsfc.nasa.gov/radhome/papers/G020802_P3_TID.pdf, February 2002.

[52] N013102_2N5114.pdf J. Titus, "NAVSEA Crane radiation test report no: NSWC C6054-2N5114-0001," http://radhome.gsfc.nasa.gov/radhome/papers/N013102_2N5114.pdf, January 2002.